

Article

Hydraulic Jump below Abrupt Asymmetric Expanding Stilling Basin on Rough Bed

Nafiseh Torkamanzad * , Ali Hosseinzadeh Dalir, Farzin Salmasi and Akram Abbaspour

Department of Water Engineering, University of Tabriz, Tabriz 5166616471, Iran

* Correspondence: n.torkamanzad@yahoo.com

Received: 22 June 2019; Accepted: 13 August 2019; Published: 23 August 2019



Abstract: The present research describes a laboratory study of hydraulic jump in the abrupt asymmetric expansion stilling basin as an energy dissipator by changing the geometry of walls and bed roughness elements. The experiments were carried out in a horizontal flume with 10 m length, 0.5 m width, and 0.5 m depth for a range of the upstream Froude numbers (Fr_1) from 5 to 11. Four physical models with expansion ratio of $\alpha = 0.33, 0.5, 0.67,$ and 1 and asymmetry ratio of $\Delta = 0.16$ were installed in the flume and two different heights of roughness elements ($h = 1.4$ and 2.8 cm) were also considered. The results indicated that the sequent depth and the jump length as well as the roller length below abrupt asymmetric expansion on the rough bed were decreased in comparison to the same parameters of the jump in a prismatic channel with smooth bed. It was revealed that the roughness elements have the effective role on stabilization of the hydraulic jump location. The analysis of energy dissipation efficiency confirmed that the spatial jump in the abruptly expanded basin with roughened bed was more efficient than classical jump. In order to estimate the hydraulic jump characteristics, empirical relationships associated with expansion ratio of basin walls, relative height of roughness elements and upstream Froude number were proposed based on the experimental data that resulted in preliminary design of an abrupt asymmetric enlarged basin.

Keywords: Asymmetric sudden expansion basin; roughened bed; hydraulic jump; energy dissipation

1. Introduction

A Hydraulic jump as a rapidly-varied flow describes a sudden transition from a supercritical flow to a subcritical flow through a strong energy dissipative mechanism [1]. The transition is characterized by a sudden rise in water-surface elevation related to the development of large-scale eddies, surface waves and spray, and air entrainment [2]. A hydraulic jump dissipates the excess kinetic energy of the flow through turbulence and converts it into energy. A hydraulic jump is extensively used in hydraulic engineering applications as an energy dissipator below chutes, weirs, gates, and spillways to protect downstream from severe scouring and possible destruction. Determining the optimum state for designing the dimensions of the stilling basin from the viewpoint of economy and safety and increasing the efficiency of hydraulic jump are considered by hydraulic engineers.

The previous investigations of a classical hydraulic jump discussed the characteristics and internal structures of the jump. Perhaps the oldest basic experimental and scientific research about hydraulic jumps was carried out by Bélanger (1828). He was the first researcher who applied continuity and momentum principles in a smooth horizontal prismatic channel to estimate sequent depth ratios [3]:

$$\frac{y_2^*}{y_1} = \frac{1}{2} \left(\sqrt{1 + 8Fr_1^2} - 1 \right) \quad (1)$$

where y_2^* is the sequent flow depth, y_1 is inflow depth and Fr_1 is inflow Froude number ($Fr_1 = v_1 / \sqrt{gy_1}$) in which v_1 is the supercritical flow velocity, and g is the acceleration due to gravity.

The first experimental data regarding the dimensionless free surface profiles were perhaps measured in 1936 by Bakhmeteff and Matzke. They found that as Froude number increases, the length and sequent depth also increase in a classical hydraulic jump [4]. For high upstream Froude numbers, Harleman (1959) indicated that the values of conjugate depth ratios were decreased in comparison with those determined by Bélanger's equation [5]. By neglecting boundary resistance, Gill [6] showed that the values of conjugate depth ratios were over predicted. Other notable studies concerning classical hydraulic jumps were done by Peterka [7], Rajaratnam [8], Hager and Bremen [9], Hager et al. [10], Wu and Rajaratnam [11] and Carollo et al. [5] and Chanson [12].

A hydraulic jump over the roughened bed was initially studied by Rajaratnam [13]. He presented a relative roughness parameter ($K = k_e / y_1$) in which k_e is the equivalent roughness [14]. Rajaratnam [13] showed that on a rough bed the tailwater depth (y_2) required to form a hydraulic jump were extremely smaller than the corresponding sequent depth estimated by Bélanger's equation (y_2^*). Additionally, Rajaratnam [13] postulated that the length of the jump on rough beds were notably shorter than that of classical jump [15]. Hughes and Flack [16] studied hydraulic jump features over roughened bed in a channel with smooth walls. They indicated that boundary roughness decreases the length and sequent depth of a jump and these reductions are related to the upstream Froude number and the degree of bed roughness. Ead and Rajaratnam [15] conducted an experimental study of the hydraulic jump on corrugated beds and specified that the reduction of the tail water depth depends on increasing of bed shear stresses, which in turn are generated by interaction of the supercritical flow with the bed corrugations. They also found that the axial velocity profiles at different cross sections in the jump were similar, with some differences from the profile of the simple plane wall jet. Carollo et al. [17] analyzed the effects of boundary roughness on the main characteristics of the hydraulic jump over the bed, roughened by gravel particles and deduced that the roller length and the sequent depth reduce with increasing roughness height. Pagliara et al. [18] carried out laboratory tests in a flume with a uniform and non-homogeneous bed material to present experimental relationships to estimate the main features of the hydraulic jump, such as roller, jump length, and sequent depth ratio. Abbaspour et al. [19] investigated the effect of sinusoidal corrugated bed with different wave steepness on the basic features of the hydraulic jump. They showed that the length ratio and the tailwater depth ratio of the jump on corrugated beds are smaller than that of the corresponding jump on a smooth bed. It was found from their research that the energy loss at the jump on a corrugated bed was 5–19% and it was about 10% for upstream Froude number more than 7. Furthermore, they indicated that the values of the bed shear stress coefficient for hydraulic jump on corrugated bed is about 10 times larger than that of a smooth bed and the analysis of velocity profiles specified that the normalized and dimensionless thickness of boundary layer was equal to 0.57 for hydraulic jump on a corrugated bed relative to corresponding value for the simple wall jet. Afzal et al. [20] studied hydraulic jump characteristics experimentally over a roughened bed in a rectangular channel. They indicated that in the inner layer the bed roughness has a passive role on imposing the wall shear stress during formation of hydraulic jump in the outer layer. They proposed analytical relations which were functions of the inflow Froude number, drag due to bed roughness and kinetic energy factor to determine conjugate depth ratio, roller length, profiles of jump depth and flow velocity. They reported that the results for a hydraulic jump over a rough bed could be directly derived from the classic jump theory by replacing the inflow Froude number with the effective inflow Froude number.

Mossa [21] studied oscillating characteristics and cyclic mechanisms of the hydraulic jumps. The results showed that the vortex roll-up process was linked to fluctuations of the longitudinal location of the jump toe. Analysis of the oscillating phenomena indicated a correlation among the surface profile elevation, velocity components and pressure fluctuations. Ben Meftah et al. [22] studied the interaction between boundary layer and shock waves in undular hydraulic jumps in a very large channel. The results showed that a sudden adverse pressure gradient occurs at the detachment point and in the flow region close to the channel sidewall. Under these conditions a separation of the boundary layer takes place and there is a detachment of the lateral shock wave. Furthermore,

their analysis of the flow velocity distributions and streamlines showed a symmetrical flow reflection towards the channel sidewalls downstream of the intersection point of the two lateral shock waves, which are reason for the trapezoidal shape of the jump.

De Padova et al. [23] studied 3D Smoothed Particle Hydrodynamics (SPH) modelling of hydraulic jump in a very large channel. The numerical simulation of the three-dimensional jump, where the hydraulic jump front is trapezoidal and the lateral shock waves induce a large recirculation region along the side walls, was compared with the results obtained in a laboratory flume on two undular jumps. The predicted velocity profiles and free-surface elevations showed a satisfactory agreement with measurements and most of the particular features of the flow, such as the trapezoidal shape of the wave front and the flow separations at the toe of the oblique shock wave along the side walls, were qualitatively and quantitatively reproduced. De Padova et al. [24] applied a Weakly-Compressible Smoothed Particle Hydrodynamics (WCSPH) scheme to the modelling of different hydraulic jumps oscillations at an abrupt drop. The numerical results showed a satisfactory agreement with the measurements and most of the particular features of the flow were qualitatively and quantitatively reproduced by the SPH model. Furthermore, the results indicated that the oscillation between the B-jump and the stronger wave-jump tends to propagate its effects more than the oscillation between wave-jump and A-jump and the waves generated by the oscillation showed a remarkably non-linear behavior while propagating in the flow direction. A 2D SPH scheme was applied to model numerically the oscillating characteristics and cyclic mechanisms in hydraulic jumps by De Padova et al. [25]. The comparison between SPH and experimental results showed an influence of different turbulence models on the amplitude spectrum and peak amplitude of the time-dependent surface elevation upstream and downstream of the hydraulic jump. The results showed that by analyzing a single cycle of the oscillating phenomena of a hydraulic jump it is possible to indicate their correlation with the vortex structures of the roller. Furthermore, analysis of the oscillating phenomena indicated a correlation among the surface profile elevations, velocity components and pressure fluctuations. Their results showed that oscillations phenomena are important for analysis of the turbulence characteristics.

Due to formation of the supercritical inflow with high velocities and intensive turbulence in a hydraulic jump, it is essential to make the stilling basin resistant to erosion and protect it from cavitation damage. Cavitation occurs in high velocity flow wherever the localized pressure is decreased due to the bed irregularities that cause a separation of flow. In order to safeguard the stilling basin from cavitation, the bed surface should be smooth or the crests of the roughness elements should be at the same elevation with the upstream bed in order not to protrude into the flow [15].

Up to now, a great number of stilling basin types has been suggested. One of the stilling basin types is a sudden enlargement of the channel width in order to improve the characteristics of hydraulic jump and increase its efficiency. Stilling basin can be designed as an abrupt symmetrical or asymmetrical expansion using appurtenances on the bed [26,27].

Herbrand [28] investigated the spatial jump in a symmetric sudden expansion with smooth bed and applied the momentum equation (by assuming hydrostatic pressure and uniform velocity distribution and neglecting the effect of turbulence, air entrainment, wall friction and the pressure force on the expansion walls) and suggested a simple empirical relation to predict the sequent depth ratio (Y); as follows:

$$\frac{Y}{Y^*} = \sqrt{\alpha} \quad (2)$$

where $\alpha = b/B$ is the expansion ratio (b is the approaching channel width and B is the enlarged channel width), $Y^* = y_2^*/y_1$ is the ratio of conjugate flow depths for the corresponding classical hydraulic jump which can be calculated by Bélanger's (1828) equation. According to the experiments of Herbrand [28], the toe of the spatial jump is located at the expansion section.

Hager [26] analyzed the hydraulic jump characteristics in a non-prismatic rectangular channel. He derived the following empirical formula based on the simplified energy equation for the relative energy dissipation of the spatial jump in terms of inflow Froude number and expansion ratio.

$$\frac{E_L}{E_1} = \left(1 - \frac{\sqrt{2\alpha}}{Fr_1}\right)^2 \tag{3}$$

where E_L/E_1 is the relative energy dissipation and E_1 is the initial energy head. The results indicated that the hydraulic jump in a symmetric abruptly enlarged channel causes higher efficiency compared with a rectangular prismatic channel for identical inflow conditions.

The spatial jump in the abrupt expansion occurs when the jump toe reaches the beginning of expansion and expands over the wider downstream basin. Occurrence of the S-jump in the sudden expanding basin can increase asymmetry of the flow, scour and develop high velocity jets along one side wall and a backward flow along the opposite basin side [27].

Bremen and Hager [29] studied transitional hydraulic jump in which the toe is located upstream from the expansion section. In their analysis, they considered an abruptly expanding rectangular channel with horizontal bed. They developed empirical equation for the sequent depth ration (Y) for T-jump based on experiments and a simplified theory.

$$\frac{Y^* - Y}{Y^* - 1} = (1 - \sqrt{\alpha})[1 - \tanh(1.9X_1)] \tag{4}$$

where X_1 is the toe position parameter ($X_1 = x_1/L_r^*$) in which x_1 is the distance between the toe of the jump and expansion section and L_r^* is the roller length of the classical hydraulic jump. They indicated that the asymmetry degree of T-jump increases notably when toe position X_1 and expansion ratio α are decreased. Additionally, they showed that the efficiency of T-jump is always larger than the corresponding classical hydraulic jump and T-jump demands less tailwater depth than classical jump. Moreover, they proposed the following equation based on their experimental results for estimating the relative energy dissipation (E_L/E_1) of T-jump in an abrupt expansion channel.

$$\frac{E_L}{E_1} = \left[1 - \frac{\sqrt{2}}{Fr_1} (1 - (1 - \sqrt{\alpha})[1 - \tanh(1.9X_1)])\right]^2 \tag{5}$$

According to Bremen and Hager [29], the S-jump takes place when the jump toe is located at the expansion section (or theoretically, when $X_1 = 0.05$). The schematic sketch of streamlines for S-jump and T-jump is shown in Figure 1.

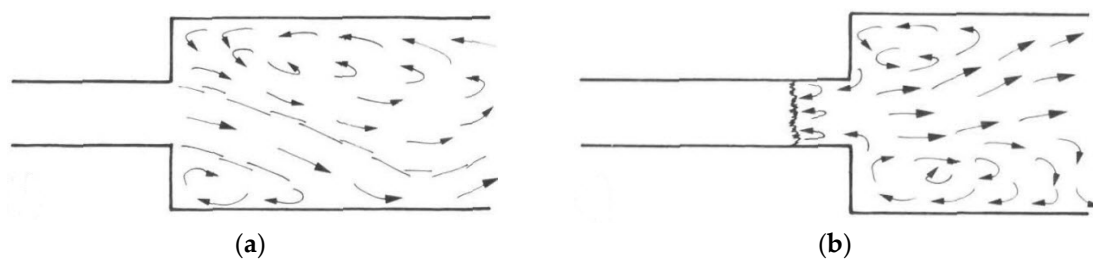


Figure 1. Schematic sketch of streamlines for (a) S-jump and (b) T-jump [29].

Alhamid [30] studied the S-jump characteristics in abrupt symmetrical expanding channels through experimental studies below different expansion ratios on smooth bed. The results indicated that compared to the classical jump, S-jumps have smaller conjugate depth ratio and higher efficiency. In addition, they observed that the efficiency of S-jump is increased by reduction of approach channel width. They obtained the prediction model for the conjugate depth ratio in horizontal bed as follows:

$$Y = \frac{1}{2} \left(\sqrt{1 + 8 [Fr_1^2 \cdot (1 + 0.25Ln\alpha)^{(1+LnFr_1)}]} - 1 \right) \tag{6}$$

They developed the prediction model for the efficiency (η) as below:

$$\frac{\eta}{\eta^*} = \left(1 - \frac{5.162Ln\alpha}{Fr_1^{1.774}} \right) \quad (7)$$

where η^* is the efficiency of the classical jump that is calculated by following Equation (1):

$$\eta^* = \left(1 - \frac{\sqrt{2}}{Fr_1} \right)^2 \quad (8)$$

More recently, the S-jump characteristics in sudden symmetric and asymmetric expanding channels by adding solid sills were studied by Zare and Doering [31]. Through their research, a new parameter, δ , that correlates sill height with sill location is introduced. They reported that this parameter can be used to control the flow and scour patterns and can assist with the basin designing. They proposed experimental regression curves and empirical equations to estimate the sequent depth, the energy dissipation, and the basin length in preliminary and operation designs of the spatial jump below abrupt symmetric and asymmetric expanding channels for two expansion ratios of $\alpha = 0.2, 0.5$ with asymmetry ratio of $\Delta = 0.22$ with different heights and locations of solid sills. They observed that the sequent depth ratio decreases by the channel asymmetry more than a symmetric expansion does it for small expansion ratios and conversely increases it for moderate to large expansion ratios. They concluded that by increasing δ , the reduction in the sequent depth is negligible for a small expansion ratio in an asymmetric channel but it increases for large expansion ratios for both symmetric and asymmetric expansions. In addition, they indicated that the energy dissipation is increased by decreasing α and increasing δ for both symmetric and asymmetric expansions; they proved that the effect of utilizing a sill on energy dissipation efficiency is reduced as inflow Froude number is increased. Their studies showed that the basin length increased by increasing the expansion ratio for symmetric expansion. As the expansion ratio increased, the basin length of asymmetric expansion channel increased more compared to the symmetric one. They derived empirical Equations (9) and (10) to determine the basin length of spatial jump for two expansion ratios of $\alpha = 0.2, 0.5$ and the range of $0 < \delta < 0.27$ for symmetric $\Delta = 0$ and asymmetric channel $\Delta = 0.22$, respectively.

$$\frac{L_j}{L_j^*} = \left[\alpha^{0.5} \text{Exp}(1 - \alpha^{0.75}) \right] + [(1 - \alpha)(0.1 + \alpha)(0.4 - 5\delta)] \quad (9)$$

$$\frac{L_j}{L_j^*} = \left[\alpha^{0.3} \text{Exp}(1 - \alpha^{0.75}) \right] + [(1 - \alpha)(0.1 + \alpha)(0.4 - 5\delta)] \quad (10)$$

Hassanpour et al. [32] studied the characteristics of the hydraulic jump in a gradually expanding rectangular stilling basin. They showed that the sequent depth ratio and relative length of the jump decreased by the decreasing divergence ratio.

The hydraulic jumps below sudden asymmetric expanding may be expected downstream of multi-gates structures like dam outlets or regulators and overflow spillway adjacent to a gated dam where parts of the gates are in operation. A hydraulic jump in an abrupt asymmetric expansion can be considered in Figure 2, where some gates are opened while others are closed. Also, hydraulic jumps in abrupt expansions can be found where the width of approaching supercritical flow is smaller compared to the width of downstream channel [31].



Figure 2. Practical sample of a hydraulic jump below abrupt asymmetric expansion [31]. Reprinted with permission from American Society of Civil Engineers (ASCE).

The spatial jump is oscillation jet flow with no specific direction and it is more effective in kinetic energy dissipation. An abrupt expanding basin not only alters the conjugate depths but also affects all other features of the jump. For designing an abrupt expanded stilling basin generally two problems remain to be solved, one is sequent depth determination and the other is the estimation of the energy dissipation [33].

Despite considerable research studies carried out about hydraulic jump on a rough bed in the rectangular stilling basin, but much attention has not properly been paid to the hydraulic jump in non-prismatic basins by using appurtenances over the bed. Design of an abrupt asymmetric expanding basin with roughened bed can improve the features of the hydraulic jump and can significantly influence the formation of symmetric flows downstream of the basin. The main purpose of this research is to study the effects of expansion ratio of the asymmetric channel and the discrete roughness elements height on the characteristics of the spatial hydraulic jump such as the sequent depth, the jump length, the roller length, the energy dissipation and the bed shear stress.

2. Methods and Materials

2.1. Laboratory Design and Measuring Instruments

The laboratory tests were performed in the hydraulic laboratory at the University of Tabriz. A rectangular channel of 0.5 m width, 0.5 m depth and 10 m length with glass side walls for observational intention was used. The schematic design of experimental setup is shown in Figure 3. The recirculation pump was used to supply water to the head tank from the storage tank. The sluice gate with a semi-circular rounded edge was generated to control the inflow conditions so that the outflow contraction was prevented, and the uniform supercritical flow depth was equal to the gate opening. The narrow section was constructed by using two vertical Plexiglas side walls that extended 1.59 m downstream to enlarge the width of the main channel abruptly and asymmetrically and connect to the main channel. The tail gate installed at the end of the channel was used to control and adjust the toe position of the spatial hydraulic jump at the abrupt expansion section. The flow rate was measured by an Acoustic flow meter that was installed on the pipeline before the head tank.

During each experimental test, the discharge and water level in the head tank were preserved steady to keep a constant Froude number at the expansion section. As the hydraulic jump was stabilized, the inflow depth at the jump toe (y_1) and the sequent depth at the end of the jump (y_2) and the free surface oscillations were measured by means of Data Logic US30 ultrasonic sensors (Datalogic company, Bologna, Italy) that were positioned over the centerline of the channel. The operation range of the sensors was 10–100 cm with an accuracy of ± 0.1 mm.

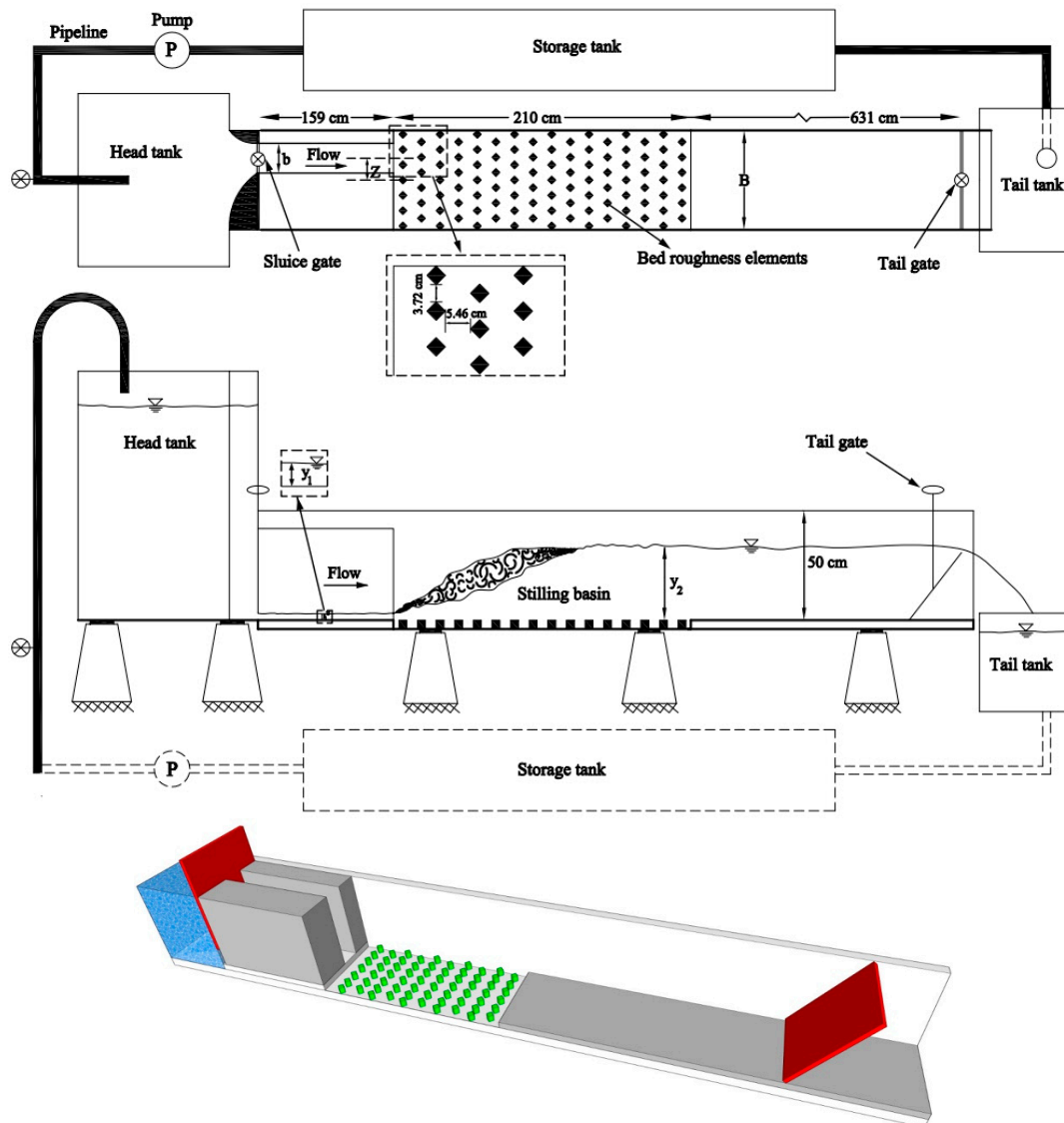


Figure 3. Plan, side, and 3D view of the experimental equipment and arrangement of the roughness elements.

Conforming to Hager [1], the hydraulic jump length (L_j) was determined between the jump toe and the location in which the gradually varied flow conditions fulfill; the roller length (L_r) is the distance between the jump toe and the roller endpoint. The jump length and the roller length were measured by a ruler with an accuracy of ± 1 mm mounted along the side walls of the channel.

Four different expansion ratios ($\alpha = b/B$) of 0.33, 0.5, 0.67 and 1 (where b is the width of the approaching channel to the sudden expansion in upstream and B is the width of the channel in downstream) were investigated. To create the asymmetric abrupt expansion, the centerline of the contraction part is eccentric from the channel centerline with a distance, Z (ranging from zero, for symmetric expansion, to the maximum possible value $Z = (B - b)/2$, where one side of the contraction section flushes with one side of the channel) as shown in Figure 3. The parameter Δ , was suggested to specify the asymmetry ratio by [31]:

$$\Delta = \frac{Z}{0.5B} \tag{11}$$

$$\Delta_{max} = 1 - \alpha \tag{12}$$

According to Equation (12), the maximum asymmetry ratio is a function of expansion ratio α , and increase in expansion ratio causes the range of the asymmetry ratio Δ , to decrease [31]. Since the maximum expansion ratio in this research is 0.67, a proposed moderate asymmetry ratio ($0 \leq \Delta \leq 0.33$) in all the experiments of the S-jump is determined to be $\Delta = 0.16$.

In order to survey the effect of roughness on the hydraulic jump characteristics on the horizontal bed (Figure 4) the discrete elements of roughness with lozenge shape made by polyethylene with two heights ($h = 1.4$ cm and 2.8 cm) were applied. According to the study conducted by Bejestan and Neisi [34], this shape of roughness elements in a staggered arrangement was more effective in decreasing of the sequent depth and length of the hydraulic jump.

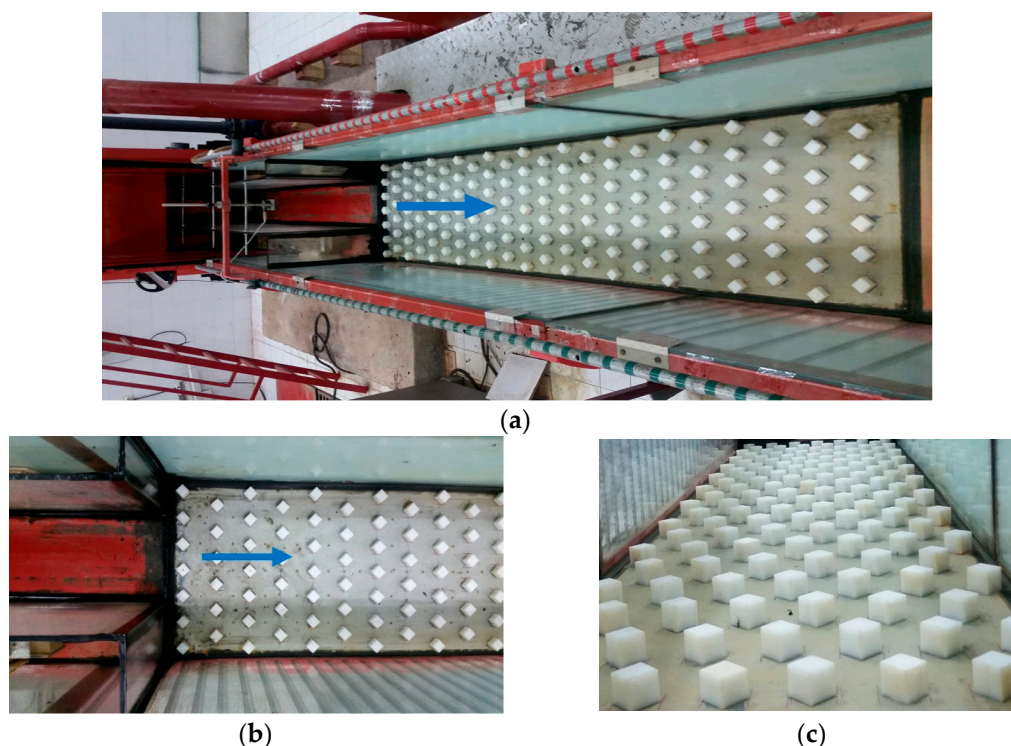


Figure 4. (a) Sketch for asymmetric expansion geometry of $\alpha = 0.5$ and roughness elements with lozenge shape. (b) Plan view of abrupt asymmetry with expansion ratio of $\alpha = 0.5$. (c) Arrangement of roughness elements with height of $h = 2.8$ cm.

The effective and optimum roughness density was obtained through preliminary experiments with different densities. The different densities were chosen according to the numbers of roughness elements, dimensions of the roughness elements and stilling basin [35]. The maximum reduction values of the sequent depth and relative length of hydraulic jump were occurred in density of 10.67% and subsequently, the effective and economical arrangement of roughness elements was in a staggered way with constant longitudinal and transverse distances and the optimum density of 10.67% (Figure 3). The crests of these roughness elements were at the same level with the upstream and downstream beds so that the roughness elements were not directly subjected to the incoming jet [34]. Hence, the protruding of the dissipative elements into the flow would be prevented and the probability of the cavitation phenomenon would be intensively decreased [15].

The upstream opening height of the gate in all the experiments was adjusted at 2.1 cm and the toe of the spatial hydraulic jump was located at the expansion section and longitudinal position of $x_1 = 1.59$ m from the upstream gate. The models of different expansion ratios with roughness elements were installed in the laboratory channel and characteristics of hydraulic jump were measured. The characteristics of the performed experiments in this investigation are shown in Table 1.

Table 1. Main parameters of the present experimental research.

Experiments	b (m)	B (m)	α	Δ	q (m^2/s)	h (m)	y_1 (m)	V_1 (m/s)	Fr_1	$Re_1 * 10^6$	y_2 (m)	L_j (m)
1	0.5	0.5	1	0.16	0.0626–0.1085	smooth bed	0.021	2.979–5.165	6.56–11.38	0.0584–0.1013	0.152–0.274	0.91–1.93
2	0.5	0.5	1	0.16	0.0628–0.1088	0.014	0.021	2.988–5.185	6.58–11.42	0.0586–0.1017	0.139–0.230	0.83–1.67
3	0.5	0.5	1	0.16	0.0622–0.1089	0.028	0.021	2.960–5.185	6.52–11.42	0.0581–0.1017	0.135–0.223	0.74–1.58
4	0.335	0.5	0.67	0.16	0.0554–0.0995	smooth bed	0.021	2.636–4.736	5.80–10.43	0.0517–0.0929	0.122–0.217	0.82–2.2
5	0.335	0.5	0.67	0.16	0.0557–0.0992	0.014	0.021	2.650–4.724	5.83–10.40	0.0520–0.0927	0.114–0.190	0.73–1.82
6	0.335	0.5	0.67	0.16	0.0553–0.0992	0.028	0.021	2.633–4.724	5.80–10.40	0.0516–0.0927	0.108–0.180	0.68–1.67
7	0.25	0.5	0.5	0.16	0.0549–0.0994	smooth bed	0.021	2.615–4.732	5.76–10.42	0.0513–0.0928	0.108–0.196	0.78–2.02
8	0.25	0.5	0.5	0.16	0.0552–0.0993	0.014	0.021	2.630–4.729	5.79–10.41	0.0516–0.0928	0.102–0.170	0.71–1.61
9	0.25	0.5	0.5	0.16	0.0554–0.993	0.028	0.021	2.638–4.725	5.81–10.41	0.0517–0.0927	0.097–0.162	0.61–1.52
10	0.165	0.5	0.33	0.16	0.0554–0.0992	smooth bed	0.021	2.687–4.724	5.81–10.41	0.0518–0.0927	0.094–0.167	0.72–1.64
11	0.165	0.5	0.33	0.16	0.0553–0.0995	0.014	0.021	2.634–4.736	5.80–10.43	0.0517–0.0929	0.090–0.146	0.64–1.36
12	0.165	0.5	0.33	0.16	0.0559–0.0992	0.028	0.021	2.663–4.722	5.86–10.40	0.0522–0.0926	0.087–0.140	0.56–1.22

Note: b and B are the upstream and downstream channel widths, α : Expansion ratio, Δ : Asymmetry ratio, q : Discharge per unit width, h : Height of the roughness elements, y_1 : Inflow depth, V_1 : Inflow mean velocity, Fr_1 : upstream Froude number, Re_1 : upstream Reynolds number, y_2 : sequent flow depth, L_j : Length of the hydraulic jump.

2.2. Dimensional Analysis

The basic factors effecting the characteristics of the hydraulic jump, such as the sequent depth (y_2) and jump length (L_j), can be defined as:

$$y_2 = f_1(\rho, \nu, g, y_1, h, V_1, b, B, Z) \quad (13)$$

$$L_j = f_2(\rho, \nu, g, y_1, h, V_1, b, B, Z) \quad (14)$$

where ρ is the density of water, ν is the kinematic viscosity of water, g is the gravity acceleration, y_1 is the inflow depth, h is the height of roughness elements, V_1 is the supercritical mean velocity, b is the width of the approaching channel, B is the width of the main channel and Z is the distance between the centerlines of the main and approaching channel. Based on the principle of Buckingham (π) theorem, the independent dimensionless relationships may be determined as:

$$\frac{y_2}{y_1} = f_3\left(Re_1 = \frac{V_1 y_1}{\nu}, Fr_1 = \frac{V_1}{\sqrt{g y_1}}, \frac{h}{y_1}, \frac{b}{y_1}, \frac{B}{y_1}, \frac{Z}{y_1}\right) \quad (15)$$

$$\frac{L_j}{y_1} = f_4\left(Re_1 = \frac{V_1 y_1}{\nu}, Fr_1 = \frac{V_1}{\sqrt{g y_1}}, \frac{h}{y_1}, \frac{b}{y_1}, \frac{B}{y_1}, \frac{Z}{y_1}\right) \quad (16)$$

where Re_1 is the upstream Reynolds number and Fr_1 is the upstream Froude number. According to the high values of upstream Reynolds number in the present tests ($52,200 \leq Re_1 \leq 101,300$), effect of viscosity is negligible [9,13]. Since the asymmetry ratio in this research is constant, the parameter Z/y_1 , is eliminated. Thus, the above equations can be written as follow:

$$\frac{y_2}{y_1} = f_5\left(Fr_1 = \frac{V_1}{\sqrt{g y_1}}, \frac{h}{y_1}, \alpha = \frac{b}{B}\right) \quad (17)$$

$$\frac{L_j}{y_1} = f_6\left(Fr_1 = \frac{V_1}{\sqrt{g y_1}}, \frac{h}{y_1}, \alpha = \frac{b}{B}\right) \quad (18)$$

2.3. Theoretical Expression

The roughened bed can increase the energy dissipation efficiency of the stilling basins. The major reason to reduce the values of y_2/y_1 and L_j/y_1 on the rough bed is the shear stress increment due to the presence of turbulent flow and larger eddies. The integrated bed shear force F_τ , acting on the horizontal and rough bed with sudden asymmetric expanding walls is determined by integral momentum principal. Momentum conservation is considered by assuming hydrostatic pressure and uniform velocity distributions; the effect of turbulence, air entrainment and wall friction are disregarded. The equation of momentum with the nomenclature of the Figure 5 may be expressed as [15,28]:

$$F_{P1} + F_e - F_{P2} - F_\tau = M_2 - M_1 \quad (19)$$

where F_{P1} , F_{P2} are the pressure force and M_1 and M_2 are the momentum flux as shown in Figure 5, and F_e represents the pressure force on the expanding side walls and it can be defined as $F_e = \frac{1}{2}\gamma(B-b)y_1^2$, in which γ is the specific weight of water [28].

The bed shear force presented by Rajaratnam [8] was defined as below [15]:

$$F_\tau = \frac{1}{2}\gamma\epsilon b y_1^2 \quad (20)$$

where ϵ is the shear force coefficient. By inserting the mentioned relations of F_e and F_τ in Equation (19), the following equation can be determined as:

$$Y^3 - Y[1 + \alpha(2Fr_1^2 - \epsilon)] + 2\alpha^2Fr_1^2 = 0 \tag{21}$$

where $Y = y_2/y_1$ is the sequent depth ratio in expanding channel.

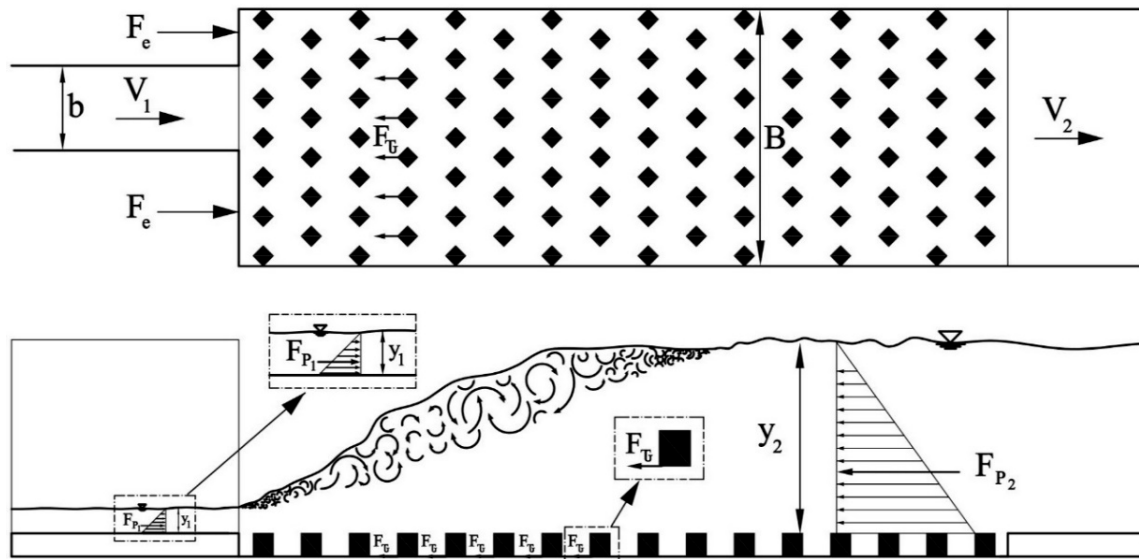


Figure 5. Schematic sketch of applying momentum equation for the hydraulic jump in abrupt asymmetric expanded channel on rough bed.

3. Results and Discussions

This research evaluates the spatial hydraulic jump below abrupt asymmetrical expansion basin with rough bed. The related parameters which must be determined for designing of the stilling basin are the sequent depth ratio, jump length and roller length, energy loss, and bed shear stress. In this section, the results are presented and discussed using dimensionless parameters.

3.1. Sequent Depth Ratio

Equation (17) indicates that the ratio of y_2/y_1 depends on the upstream Froude number (Fr_1), the relative roughness height (h/y_1) and the expansion ratio ($\alpha = b/B$). The values of y_2/y_1 are plotted versus Fr_1 in Figure 6 for different expansion ratios on the horizontal bed and asymmetric case to evaluate the effect of roughness height on the sequent depth ratio. Additionally, to survey the effect of the expansion ratio Figure 6 compares the sequent depth ratios with Equations (2), (4) and (6) proposed by Herbrand [28], Bremen and Hager [29] and Alhamid [30] for the S-jump in sudden symmetric expanding channels, respectively.

Considering the Figure 6, in all experiments the sequent depth values increased by increasing Fr_1 values and decreased by decreasing the expansion ratio. In comparison with the previous research in sudden symmetric expanding channels, the results showed that the asymmetry of the expanding channel decreased the sequent depth ratio. It can be seen from Figure 6 that in all expansion ratios, the sequent depth ratios on the rough bed were decreased compared to the classical hydraulic jump which is directly related to both the asymmetry expanding of the channel and height of roughness elements.

The sequent depth values (y_2/y_1) also decreased as the roughness height increased. In the experiments, eddies and flow separation may be formed between the dissipative elements due to the increasing of roughness height and resulted in the reduction of sequent depth values. In all sudden

expansion ratios, the sequent depth ratio for the S-jump in abrupt asymmetric expanding with smooth and rough bed was smaller than that of the corresponding classical jump. This indicates that both expansion ratio and roughness elements play an important role to reduce the sequent depth values.

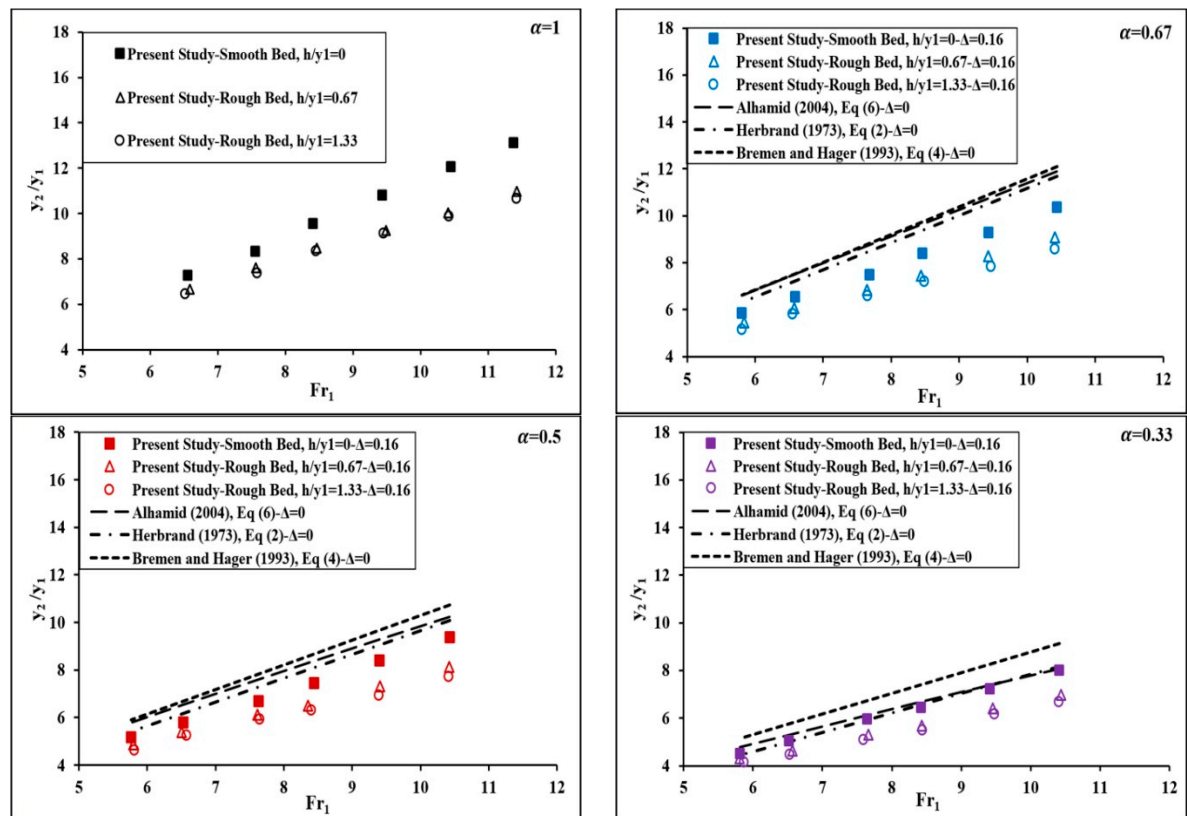


Figure 6. Sequent depth ratio as a function of upstream Froude number for two relative roughness heights ($h/y_1 = 0.67$ and 1.33) and different expansion ratios ($\alpha = 0.33, 0.5, 0.67, 1$) with asymmetry ratio of $\Delta = 0.16$.

The regression-based relationship between y_2/y_1 , Fr_1 , and four asymmetric expansion ratios with two roughness heights can be determined by the Equation (22) with a determination coefficient (R^2) equal to 0.962.

$$\frac{y_2}{y_1} = 0.797(Fr_1) - 0.855\left(\frac{h}{y_1}\right) + 4.097(\alpha) - 1.388 \quad (22)$$

The Equation (22) indicates that the sequent depth ratio increases with the increase of expansion ratio and upstream Froude number, sequent depth values also decrease with the increase of relative height of roughness elements.

Figure 7 shows the comparison between the measure sequent depth ratio in sudden asymmetric expanding channel from the present study and those predicted by Equations (2), (4), (6) and (22). The results indicate that the computed values by Equations (2), (4), (6) and (22) have $\pm 19\%$ difference with the observed values. Figure 7 shows that Equation (22) of the present study predicts y_2/y_1 accurately, while Equations (2), (4) and (6) generally overestimate the sequent depth ratio compared with the present measured data and some data fall on error line $+19\%$ due to the asymmetry expanding of the channel and bed roughness elements in the present study.

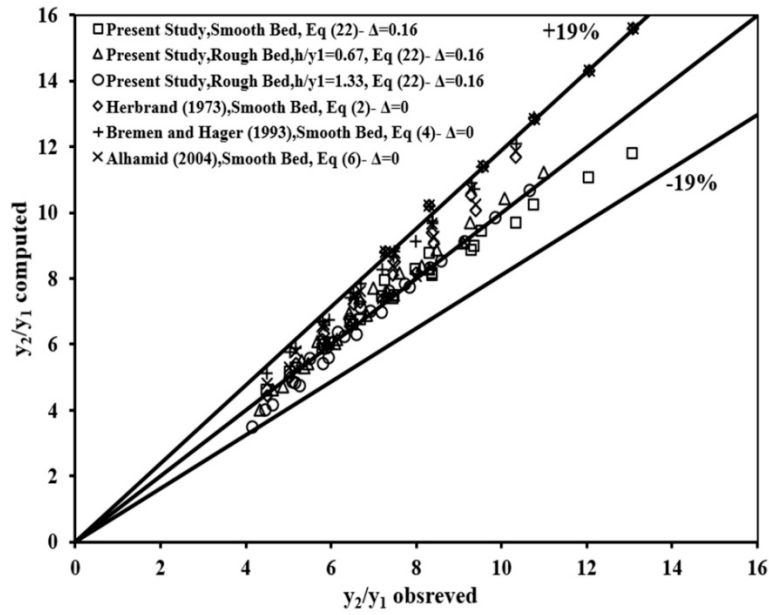


Figure 7. Comparison of the computed values of y_2/y_1 by different prediction equations with the present observed data.

The comparison between the observed y_2/y_1 data in the present research and data obtained by Ead and Rajaratnam [15] and Carollo et al. [17], and the values computed by Equation (22) are shown in the Figure 8.

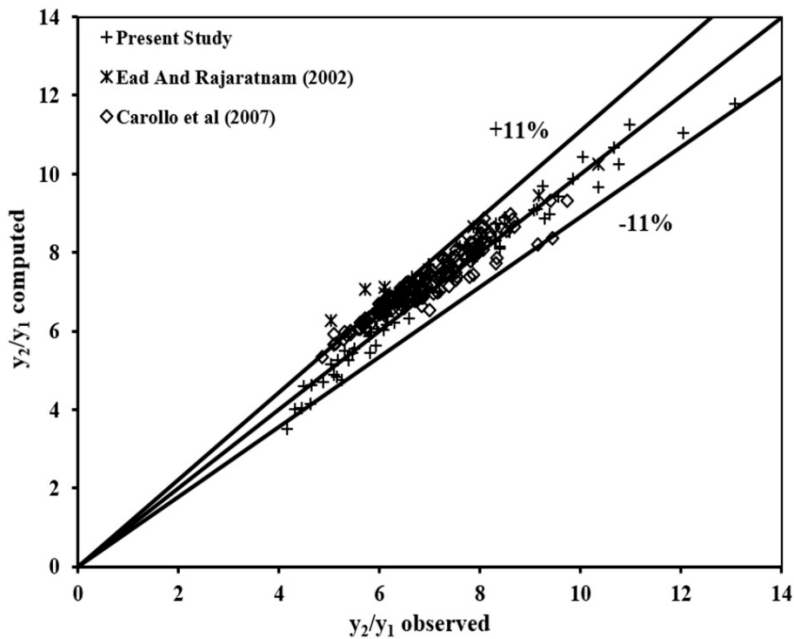


Figure 8. Comparison between the observed y_2/y_1 values with those obtained by Equation (22).

As shown in Figure 8, the computed data are close to the agreement line and indicate a $\pm 11\%$ difference with the observed data. Using Equation (22) to compute y_2/y_1 values indicates a good agreement with the previous research and only 7 out of 233 data fall beyond the error band $\pm 11\%$.

To evaluate the reduction of the sequent depth, Ead and Rajaratnam [15] defined the non-dimensional depth deficit parameter, D , as $D = (y_2^* - y_2)/y_2^*$. In this equation, y_2^* refers to the sequent depth on a smooth bed with the same upstream conditions. The variation of D with

Fr_1 for the observed values is showed in Figure 9. Figure 9 shows that D values increase by the decreasing of the expansion ratio and increasing of the roughness elements height. The results indicate that the effect of expansion ratio on the non-dimensional depth deficit parameter increase in small expansion ratios. As it can be seen in the Figure 9, the range of D values in expansion ratios of $\alpha = 0.67$, $\alpha = 0.5$ and $\alpha = 0.33$ on rough bed with $h/y_1 = 1.33$ are $17.85 \leq D\% \leq 28.11$, $26.45 \leq D\% \leq 35.23$ and $34.61 \leq D\% \leq 43.96$, respectively, and the maximum decrement of sequent depth is obtained for the expansion ratio of $\alpha = 0.33$ and roughened bed with the relative height of $h/y_1 = 1.33$.

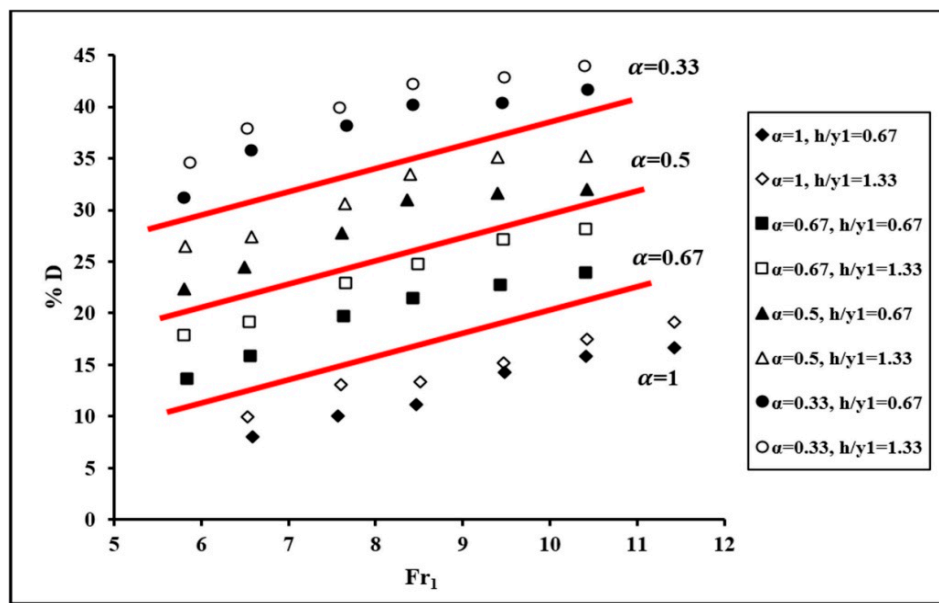


Figure 9. Non-Dimensional depth deficit D , versus Fr_1 .

The average percentage reduction of sequent depth ($D\%$) for experiments is presented in Table 2. The present research indicates that the decrement of sequent depths in the abruptly asymmetric expanding stilling basin is greater than those obtained in the classical jump.

Table 2. The range and mean reduction of sequent depth ($D\%$).

Experiments		$D\%$	$\bar{D}\%$
α	h/y_1		
1	0.67	$8.03 \leq D \leq 16.66$	12.66
1	1.33	$9.95 \leq D \leq 19.14$	14.71
0.67	0.67	$13.7 \leq D \leq 23.92$	19.55
0.67	1.33	$17.85 \leq D \leq 28.11$	23.33
0.5	0.67	$22.32 \leq D \leq 31.96$	28.21
0.5	1.33	$26.45 \leq D \leq 35.23$	31.38
0.33	0.67	$31.16 \leq D \leq 41.62$	37.88
0.33	1.33	$34.61 \leq D \leq 43.96$	40.22

3.2. Relative Length

The major purpose of applying rough bed in an abruptly expanding stilling basin is to decrease the jump length and avoiding the asymmetry of the flow and stabilization of the jump in position. Additionally, these roughness elements stabilize the S-jump position and avoid jump runoffs toward the downstream region. The relation between L_j/y_1 and Fr_1 values for different expansion ratios on smooth and roughened bed, are plotted in Figure 10. In this Figure, the comparison of the relative lengths of spatial jump introduced by Zare and Doering [31] in the symmetric expanding channel as

the Equation (9) was also made. Moreover, the following Equations (23) and (24) defined by Hager [1] and USBR [36], respectively, were used to compare the relative lengths of a classical jump with the present experimental data.

$$\frac{L_j}{y_1} = 220 \tan h\left(\frac{Fr_1 - 1}{22}\right) \tag{23}$$

$$\frac{L_j}{y_1} = 6 \frac{y_2}{y_1} \tag{24}$$

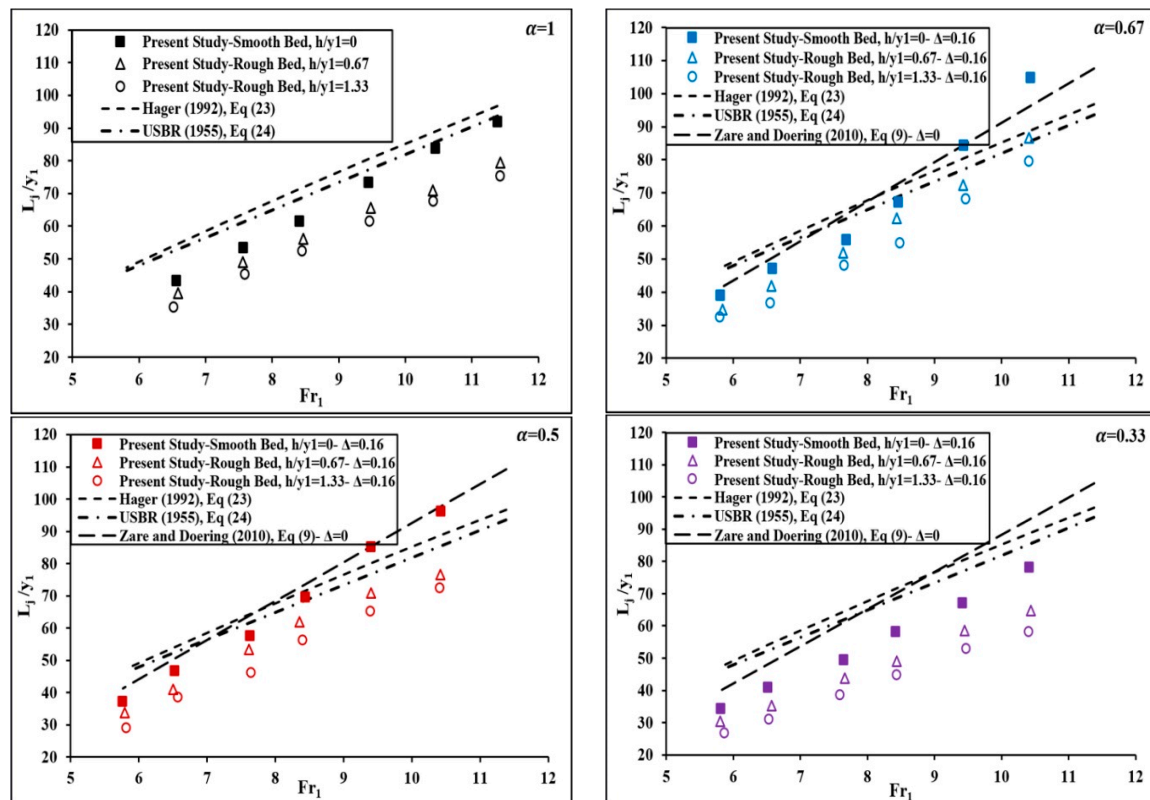


Figure 10. Relative length of the hydraulic jump as a function of upstream Froude number for two relative roughness heights ($h/y_1 = 0.67$ and 1.33) and different expansion ratios ($\alpha = 0.33, 0.5, 0.67, 1$) with asymmetry ratio of $\Delta = 0.16$.

As shown in Figure 10, the L_j/y_1 values increase with the increase of Fr_1 . The experimental results demonstrated that the roughness effect on the length of S-jump in asymmetric sudden expanding channel is considerable and results in the stabilization of the jump and notable reduction of the jump length. From Figure 10, it is noticed that the roughness with 2.8 cm height is more effective in reducing the L_j/y_1 values compared with the other height of roughness elements. Figure 10 indicates that the relative length values of S-jump decrease compared with a classical hydraulic jump (Equations (23) and (24)) due to the effects of sudden asymmetry expanding of the channel and bed roughness elements. The results in Figure 10 show that the relative length data of S-jump in an abrupt asymmetric expanding channel with roughened bed decrease compared with the symmetric one (Equation (9)) due to the effect of roughness elements.

Furthermore, in Figure 11, the values of the relative length of the hydraulic jump (L_j/y_1) obtained below abrupt asymmetrical enlargement stilling basin with different expansion ratios ($\alpha = 0.33, 0.5, 0.67, 1$) on smooth and rough bed ($h/y_1 = 1.33$) are compared with those obtained by Hager [1], United States Bureau of Reclamation (USBR) [36] and Zare and Doering [31].

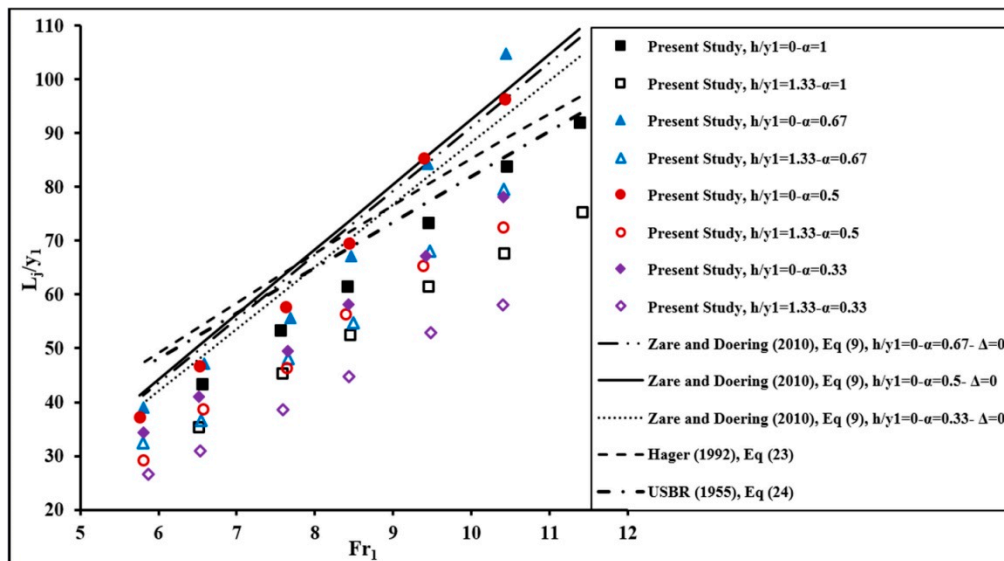


Figure 11. Relative length of the hydraulic jump as a function of upstream Froude number for different expansion ratios ($\alpha = 0.33, 0.5, 0.67, 1$) with asymmetry ratio $\Delta = 0.16$ on smooth and rough bed ($h/y_1 = 1.33$).

According to experimental results in Figures 10 and 11, the length of the hydraulic jump in abruptly expanding channel with expansion ratios of $\alpha = 0.67$ and $\alpha = 0.5$ was greater than the jump in expansion ratios of $\alpha = 0.33$ and $\alpha = 1$. The hydraulic jump extending to the downstream of the channel was mainly due to the asymmetry of the S-jump, the turbulence, pulsating and instability of the flow. Figure 11 shows that in asymmetric expansion channel the relative length decreases by the decreasing the expansion ratio. The results also indicate that installing the roughness elements decrease the asymmetry of the flow and stabilize the S-jump and significantly affect the length of the hydraulic jump.

The empirical relationship for the relative length of the jump (L_j/y_1) with its dominant parameters Fr_1, α and h/y_1 , is derived by the following regression equation with R^2 equal to 0.958.

$$\frac{L_j}{y_1} = -87.569(\alpha)^2 + 122.142(\alpha) + 3.68\left(\frac{h}{y_1}\right)^2 - 14.635\left(\frac{h}{y_1}\right) + 9.833(Fr_1) - 54.58 \quad (25)$$

As it is displayed in Figure 12, for all the experiments the values of relative length ratio (L_j/y_1) computed by Equation (25) are compared with those of observed values. The Figure 12 also indicates that the results obtained by the above equation show $\pm 18\%$ difference with the corresponding observed values.

Table 3 shows the comparison of the variations of the jump length in different expansion ratios on smooth and rough beds with classical jump. This Table shows that the increasing value of the jump length in expansion ratios of $\alpha = 0.67$ and $\alpha = 0.5$ on smooth bed are 11.71% and 11.2%, respectively due to occurrence of instabilities at the S-jump in sudden expansion. In addition, the results show that the decreasing value of the jump length in expansion ratios of $\alpha = 0.67, \alpha = 0.5$, and $\alpha = 0.33$ on rough bed with $h/y_1 = 1.33$ are 9.7%, 12.6%, and 27.92%, respectively. The results in Table 3 indicate that the effect of expansion ratio on the reduction of relative length of jump increased in small expansion ratios especially on the roughened bed with the relative height of $h/y_1 = 1.33$.

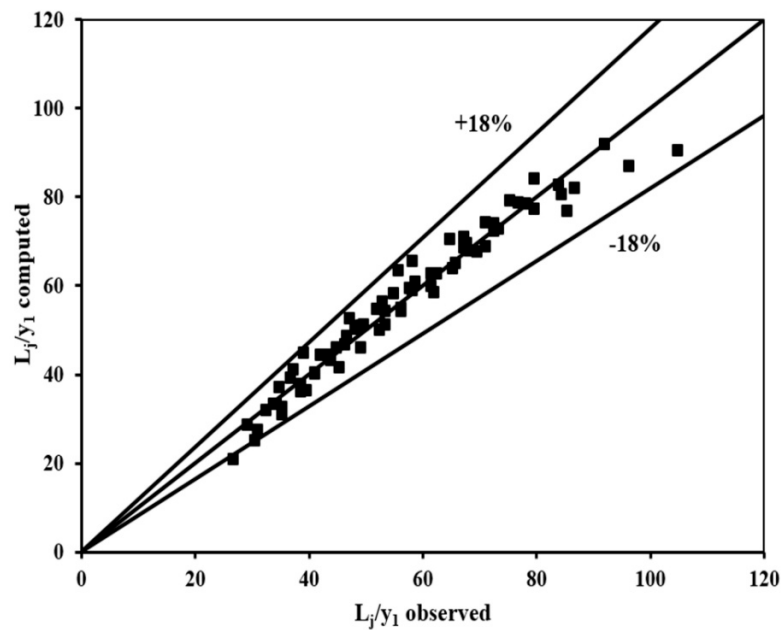


Figure 12. Comparison between the observed values of L_j/y_1 in this research and those computed by Equation (25).

Table 3. Comparison of variations percentage of the hydraulic jump length to the classical jump.

Experiments		$(1 - \frac{L_j}{L_j}) \times 100$
α	h/y_1	
1	0.67	-11.05
1	1.33	-17.13
0.67	0	+11.71
0.67	0.67	-0.91
0.67	1.33	-9.7
0.5	0	+11.2
0.5	0.67	-2.96
0.5	1.33	-12.6
0.33	0	-5.98
0.33	0.67	-19.13
0.33	1.33	-27.92

The + and – signs represent an increasing and decreasing of hydraulic jump length compared to the classical jump.

3.3. Relative Roller Length

Previous experimental investigations by Carollo et al. [17], Hager et al. [10], Pietrkowski (1932), and Smetana (1937) proposed that the roller length (L_r), as the distance between the jump toe and the place where the roller ends, was a better length parameter than the jump length since it was relatively easy to observe and can properly be specified for steady flow conditions [37]. The length of the jump is difficult to describe due to the surface waves, the turbulence and oscillating flow at the end of hydraulic jump [37].

The laboratory investigations of Pietrkowski (1932), Smetana (1937), Hager [1] and Carollo and Ferro (2004) proposed the following relationship for the roller length which is proportional to the difference between the sequent depths for the jump on smooth and rough beds [17].

$$\frac{L_r}{y_1} = a \left(\frac{y_2}{y_1} - 1 \right) \tag{26}$$

where a is the coefficient depending on experimental conditions and equal to 4.616 as determined by Carollo et al. [17].

Carollo and Ferro (2004) suggested the following equations for the relative roller length and verified applicability of these equations by using the roller length data for the smooth and rough beds by Ead and Rajaratnam [15], Hughes and Flack [16] and Hager et al. [10].

$$\frac{L_r}{y_1} = a_0 \left(\frac{y_1}{y_2} \right)^{-1.272} \tag{27}$$

$$\frac{L_r}{y_1} = b_0 (Fr_1 - 1) \tag{28}$$

where a_0 and b_0 are numerical coefficients depending on bed roughness and equal to 2.244 and $6.525 \exp(-0.6 \frac{h}{y_1})$, respectively, as determined by Carollo et al. [17].

In order to investigate the influence of roughness height and the expansion ratio, the values of the relative roller length (L_r/y_1) versus the upstream Froude number (Fr_1) are presented in Figure 13. The results of this research for the relative roller length with different expansion ratios and roughness heights are compared with the Equations (26)–(28) proposed by Carollo et al. [17] on rough bed with $h/y_1 = 1.33$ in rectangular channel. In these Figures, the relative roller lengths of a classical jump calculated by Equation (29) suggested by Hager et al. [10] are also compared.

$$\frac{L_r}{y_1} = -12 + 160 \tanh\left(\frac{Fr_1}{20}\right) \tag{29}$$

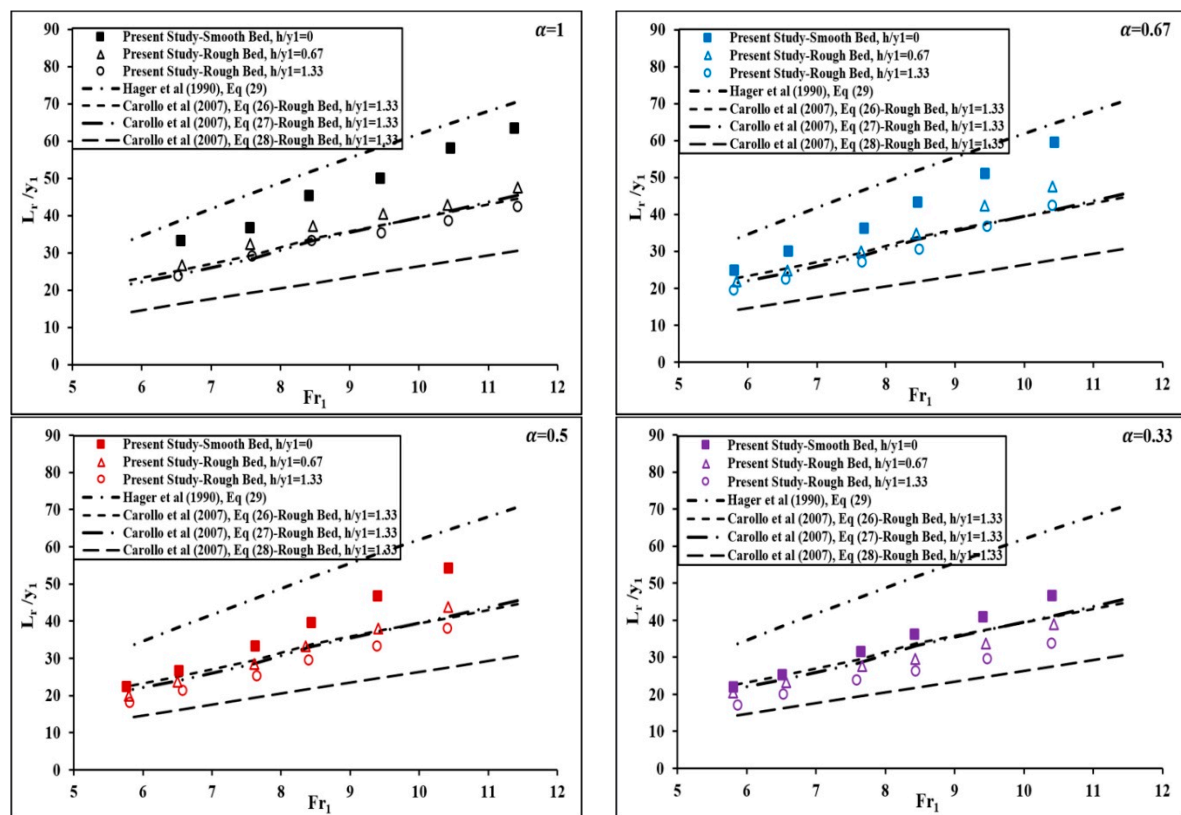


Figure 13. Relative roller length of the hydraulic jump as a function of upstream Froude number for two relative roughness heights ($h/y_1 = 0.67$ and 1.33) and different expansion ratios ($\alpha = 0.33, 0.5, 0.67, 1$) with asymmetry ratio of $\Delta = 0.16$.

Figure 13 indicates that the relative roller length values of S-jump decrease compared with a classical jump due to the effects of sudden asymmetry expanding of the channel and roughness elements and as a result Equation (29) overestimates the relative roller length compared with the present measure data. As shown in Figure 13, the relative roller length of the jump decreases by the increase of roughness ratio and increases when the expansion ratio and upstream Froude number are increased.

The equation based on the regression analysis with a value of R^2 equal to 0.949 is determined to show the effect of roughness elements and expansion ratios with different Fr_1 values on the roller length.

$$\frac{L_r}{y_1} = -20.442(\alpha)^2 + 35.992(\alpha) + 3.373\left(\frac{h}{y_1}\right)^2 - 1.639\left(\frac{h}{y_1}\right) + 5.127(Fr_1) - 15.836 \quad (30)$$

Figure 14 shows a comparison of the observed values of L_r/y_1 in this study with the values computed by Equation (30). It is found that the computed data by Equation (30) indicate a $\pm 16\%$ difference with the observed values in this research.

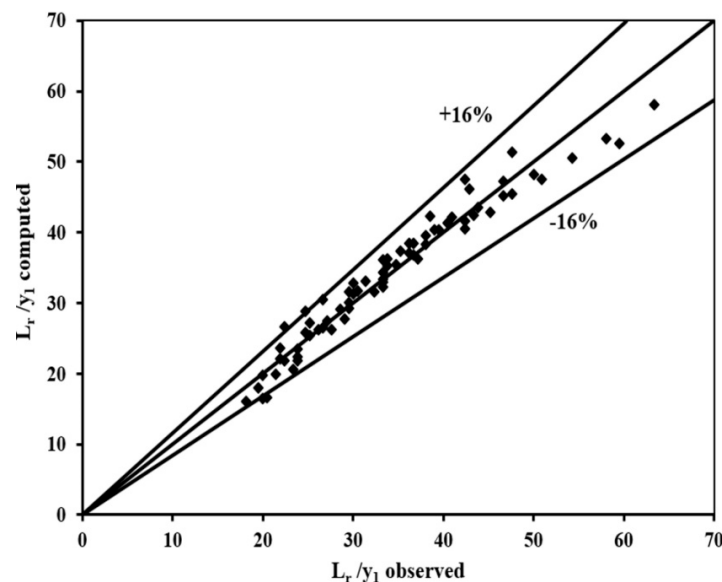


Figure 14. Comparison of the observed values of L_r/y_1 with those computed by Equation (30).

The roller length data obtained experimentally from this research are used to examine the applicability of Equations (26)–(28). For different expansion ratios and roughness heights, the experimental pairs $(L_r/y_1, y_2/y_1 - 1)$, $(L_r/y_1, y_1/y_2)$, and $(L_r/y_1, Fr_1 - 1)$ values are plotted in Figure 15a,b and Figure 16, respectively. According to Figure 15, a single relationship independent of the roughness height and expansion ratio between the pairs of $(L_r/y_1, y_2/y_1 - 1)$ and $(L_r/y_1, y_1/y_2)$ can be determined but Figure 16 indicates that a single relationship may not be obtained using the pairs $(L_r/y_1, Fr_1 - 1)$, as it was already revealed by Carollo et al. [17].

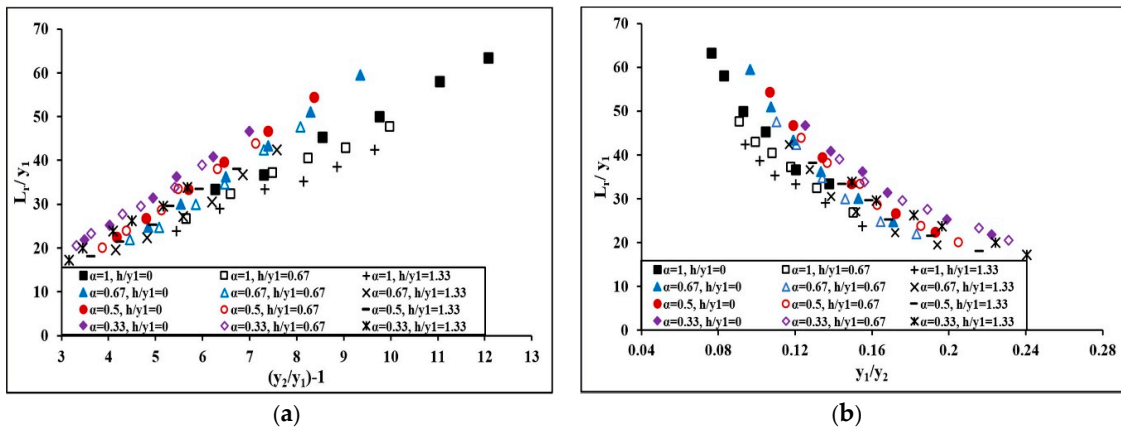


Figure 15. Relation between the ratio of L_r/y_1 and (a) the difference $(y_2/y_1 - 1)$, (b) the ratio of (y_1/y_2) for the experimental data of this research.

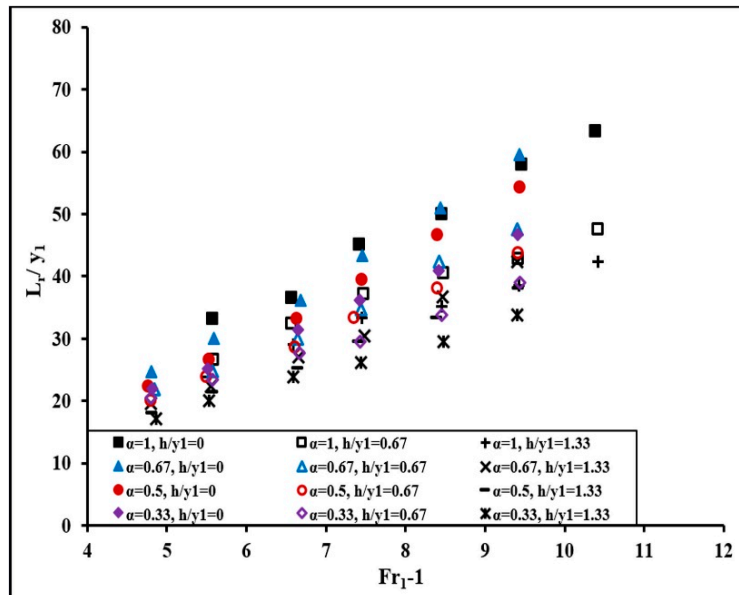


Figure 16. Relation between the ratio of L_r/y_1 and $(Fr_1 - 1)$ for the experimental data of this research.

Table 4 shows the computed coefficients a , a_0 , and b_0 , for different expansion ratios ($\alpha = 1, 0.67, 0.5$ and 0.33) and roughness heights. The values of coefficients a , a_0 , and b_0 calculated with the data of Hager et al. [10] and Hughes and Flack [16] by Carollo and Ferro (2004) as well as the values of a , a_0 , and b_0 determined by Carollo et al. [17] are also presented in Table 4. Due to the dependence of the coefficients a and a_0 , on sequent depth ratio, the difference between the values of coefficients a and a_0 in the present study and those estimated by other researchers in prismatic channels showed a significant reduction of sequent depth ratio in abruptly asymmetric expanding channels.

Table 4. Values of a , a_0 , and b_0 coefficients obtained from the experimental data of this research and determined by the previous investigations. Reprinted with permission from ASCE.

Experimental Research	α	h (cm)	a	a_0	b_0
Hughes and Flack [16]	1	0	5.06	2.42	6.58
Carollo et al. [17]	1	0	4.12	2.04	5.73
Present Study	1	0	5.28	2.21	6.47
Present Study	0.67	0	7.69	3.43	7.50
Present Study	0.5	0	7.64	3.51	6.89
Present Study	0.33	0	7.16	3.43	5.41
Hughes and Flack [16]	1	0.32	4.53	2.25	5.90
Carollo et al. [17]	1	0.46	4.26	2.15	5.02
Hughes and Flack [16]	1	0.49	4.66	2.33	6.00
Hughes and Flack [16]	1	0.61	4.06	2.00	4.92
Hughes and Flack [16]	1	0.64	4.43	2.22	5.44
Carollo et al. [17]	1	0.82	3.92	1.98	4.67
Hughes and Flack [16]	1	1.04	4.07	2.01	4.79
Present Study	1	1.4	4.69	2.04	4.12
Present Study	0.67	1.4	7.35	3.38	5.79
Present Study	0.5	1.4	7.38	3.49	5.11
Present Study	0.33	1.4	6.63	3.26	3.88
Carollo et al. [17]	1	1.46	3.86	1.94	4.16
Present Study	1	2.8	4.21	1.84	3.62
Present Study	0.67	2.8	6.73	3.14	4.92
Present Study	0.5	2.8	6.64	3.19	4.34
Present Study	0.33	2.8	6.27	3.12	3.52

Fitting Equations (26) and (27) to all experimental data obtained from this research gives $a = 4.963$ and $a_0 = 2.227$. Therefore, Equations (31) and (32) for this study can be written as:

$$\frac{L_r}{y_1} = 4.963 \left(\frac{y_2}{y_1} - 1 \right), \quad R^2 = 0.839 \tag{31}$$

$$\frac{L_r}{y_1} = 2.227 \left(\frac{y_1}{y_2} \right)^{-1.272}, \quad R^2 = 0.834 \tag{32}$$

Considering Equation (31), as the values of $(y_2/y_1 - 1)$ increase, the ratios of L_r/y_1 increases linearly and the Equation (32) also indicates that the values of L_r/y_1 decrease exponentially with the increase of (y_1/y_2) values.

The experimental values of L_r/y_1 in the present research, Carollo et al. [17] and Ead and Rajaratnam [15] are compared with the values computed by Equations (31) and (32) in the Figure 17a,b, respectively. The Figure 17 indicates that the results obtained by the Equation (31) show $\pm 26\%$ variation with the corresponding observed data. Additionally, the difference between the computed data of L_r/y_1 by Equation (32) and the experimental data of present research, Ead and Rajaratnam [15] and Carollo et al. [17] are in the range of $\pm 30\%$ and only 9 out of the 356 L_r/y_1 ratios fall beyond the mentioned error band.

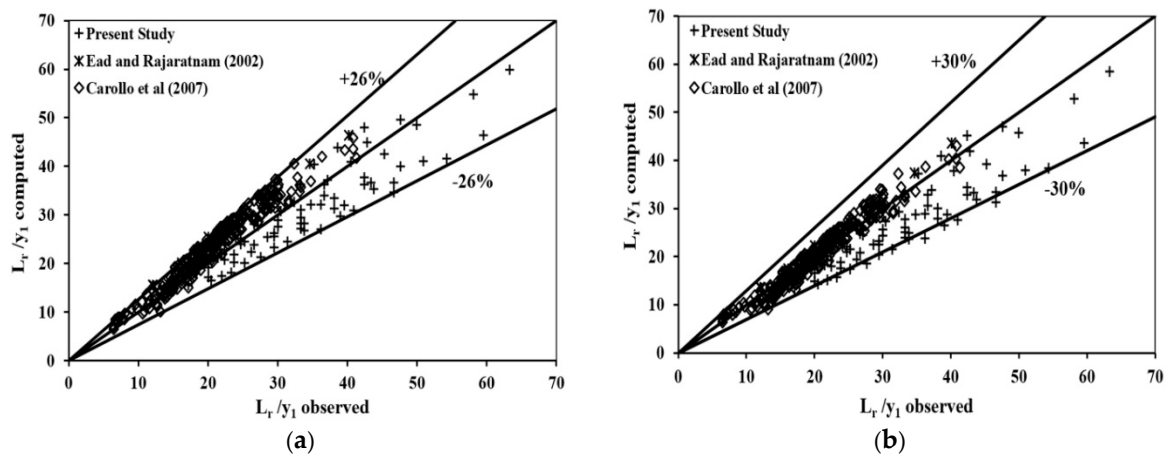


Figure 17. Comparison between the experimental values of the ratio L_r/y_1 and (a) values computed by Equation (31), (b) values computed by Equation (32).

The following regression-based equation is defined between the estimated b_0 values, the expansion ratio and the relative roughness height.

$$b_0 = 2.227 \exp\left(-0.772 \frac{h}{y_1}\right) - 2.279(\alpha)^2 + 4.33(\alpha) + 1.499, \quad R^2 = 0.889 \quad (33)$$

Application of Equation (28) indicated that the coefficient b_0 , is related to the relative roughness height and expansion ratio. Then the following equation was determined by substituting Equation (33) in Equation (28):

$$\frac{L_r}{y_1} = \left[2.227 \exp\left(-0.772 \frac{h}{y_1}\right) - 2.279(\alpha)^2 + 4.33(\alpha) + 1.499 \right] (Fr_1 - 1) \quad (34)$$

As it can be seen from Figure 18, comparing the observed values of L_r/y_1 in this study, Ead and Rajaratnam [15] and Carollo et al. [17] and those computed by Equation (34) indicate $\pm 25\%$ difference.

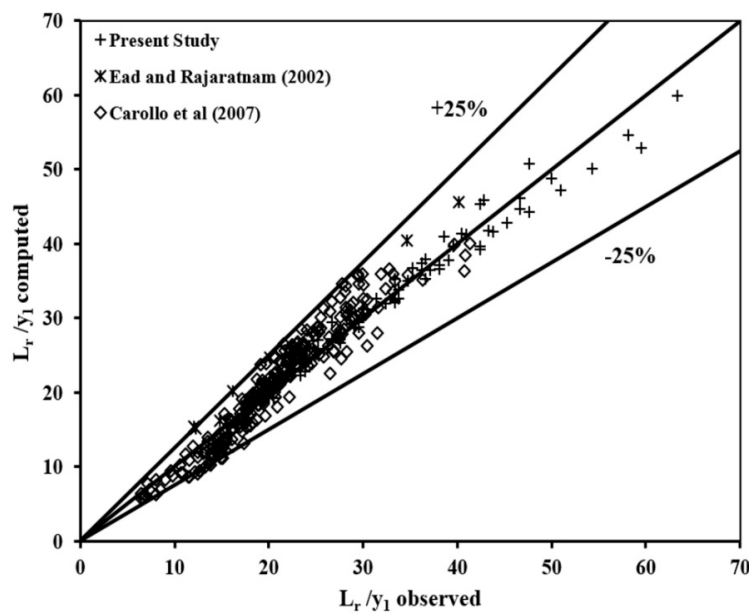


Figure 18. Comparison between the experimental values of the ratio L_r/y_1 and the values computed by Equation (34).

3.4. Energy Loss

The loss of energy which takes place in the jump (E_L) is defined by the specific energy equation as below:

$$E_L = E_1 - E_2 = \left(y_1 + \frac{V_1^2}{2g} \right) - \left(y_2 + \frac{V_2^2}{2g} \right) \tag{35}$$

where E_1 and E_2 are the specific energy at the rapid upstream flow and tranquil downstream flow, respectively. The relative energy loss of the jump in abruptly expanding channel is determined by applying both the continuity and the specific energy equations:

$$\frac{E_L}{E_1} = \frac{y_1 - y_2 + \frac{Fr_1^2 y_1}{2} \left(1 - \left(\frac{A_1}{A_2} \right)^2 \right)}{y_1 + \frac{Fr_1^2 y_1}{2}} \tag{36}$$

where E_L/E_1 is the relative energy loss. The experimental values of E_L/E_1 below abrupt asymmetrical expanding channel are computed by Equation (36) for different expansion ratios with two relative roughness heights; the relative energy dissipation data are plotted as a function of Fr_1 in Figure 19. In addition, Equations (3), (5) and (7) defined by Hager [26], Bremen and Hager [29] and Alhamid [30], respectively, for the S-jump in sudden symmetric expanding channels, are shown in the Figure 19 for comparison.

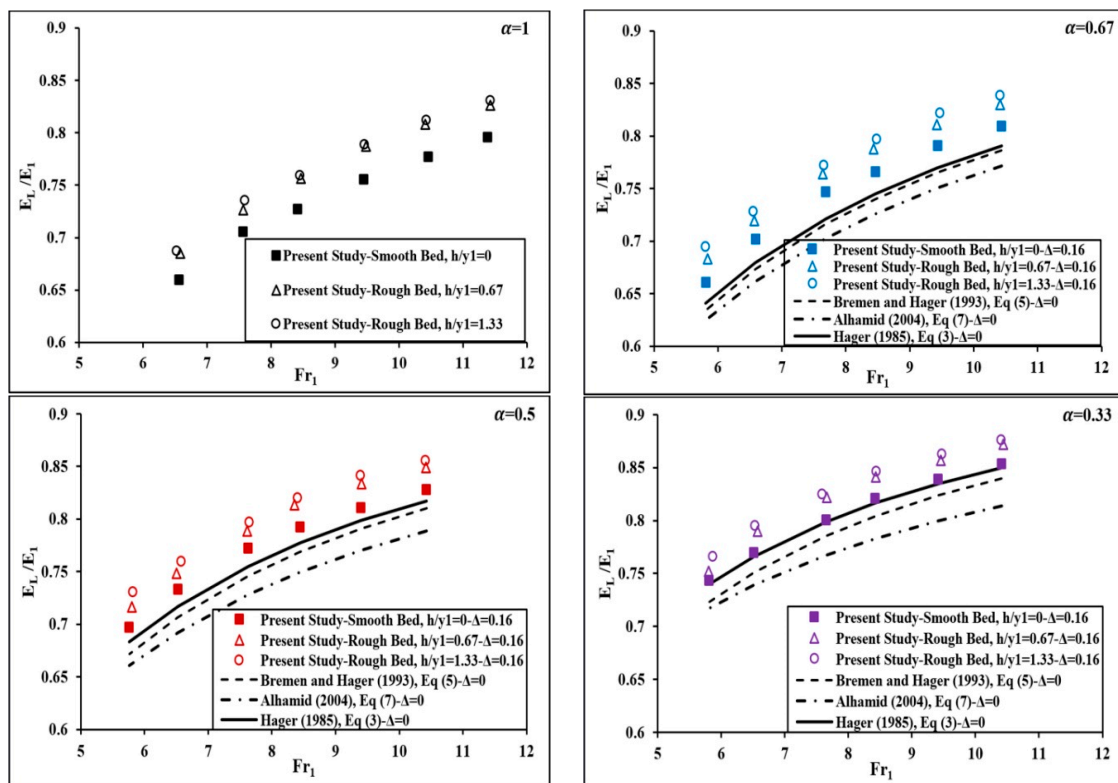


Figure 19. Relative energy loss of the hydraulic jump as a function of upstream Froude number for two relative roughness heights ($h/y_1 = 0.67$ and 1.33) and different expansion ratios ($\alpha = 0.33, 0.5, 0.67, 1$) with asymmetry ratio of $\Delta = 0.16$.

It can be observed from Figure 19 that for the same Fr_1 , the relative energy dissipation (E_L/E_1) values in all abruptly expanded channels on roughened beds are greater than those determined in smooth bed; as a result, the S-jump in abruptly expanded stilling basin on roughened bed is more efficient than the same jump on smooth bed.

Additionally, Figure 19 indicates that the relative energy loss for the jump in all expansion ratios of side walls is greater than the values obtained from classical jump. As shown in the Figure 19, in all experiments the values of the relative energy loss increase with the increase of Fr_1 values. Moreover the values obtained from each model in these Figures indicate that as the roughness height increases, the relative energy loss increases due to generation of the larger eddies between roughness elements. In comparison with the previous research in sudden symmetric expanding basins, the results revealed that the asymmetry of the expanding channel with roughened bed increased the relative energy dissipation.

The effects of different expansion ratios on the values of E_L/E_1 at the smooth and rough bed are compared with each other in Figure 20. The Figures postulate that the values of E_L/E_1 increase as the expansion ratios decrease. Also, the results obtained indicate that the energy dissipation efficiency in the jump with the expansion ratio of $\alpha = 0.33$ and relative roughness height of $h/y_1 = 1.33$ is 82.85%. Therefore, this type of basin is more effective in dissipation of the excess energy of the jump. The high efficiency of this basin is probably due to the presence of large eddies along the roller length of the basin.

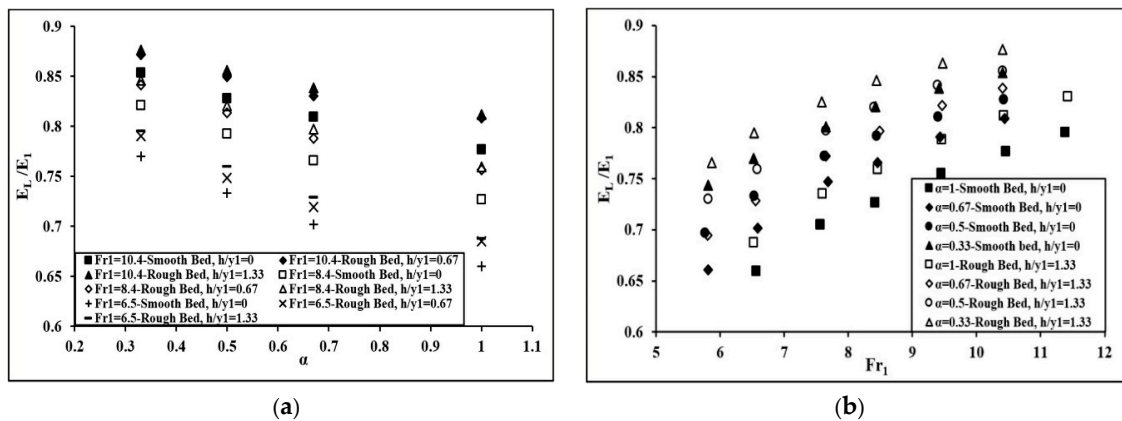


Figure 20. Variation of energy dissipation on the smooth and rough bed (a) with expansion ratios for different upstream Froude numbers, (b) with upstream Froude numbers for different expansion ratios.

The following empirical equation obtained by non-linear regression with the value of $R^2 = 0.98$ may be used to predict the relation between the relative energy loss (E_L/E_1), the upstream Froude number (Fr_1), the expansion ratio (α) and the relative roughness height (h/y_1).

$$\frac{E_L}{E_1} = 0.229Ln(Fr_1) + 0.102(\alpha)^2 - 0.267(\alpha) + 0.021\left(\frac{h}{y_1}\right) + 0.408 \tag{37}$$

Equation (37) shows that as the expansion ratio increases the relative energy loss decreases. Additionally, the relative energy loss is directly dependent on the relative roughness height and the logarithmic value of the upstream Froude number.

3.5. Hydraulic Jump and Bed Shear Stress

Bed shear stress increment is the major reason for reduction of the sequent depth and jump length. As a result, the investigation of the shear stress on the bed is important. It is usually described by shear stress coefficient (ε). The following shear stress equations were introduced by Ead and Rajaratnam [15] for the smooth and rough beds, respectively:

$$\varepsilon = 0.16Fr_1^2 - 0.8Fr_1 + 1, \quad R^2 = 1 \tag{38}$$

$$\varepsilon = (Fr_1 - 1)^2, \quad R^2 = 1 \tag{39}$$

To show the effect of roughness elements and expansion ratio on shear stress coefficient, the values of index ε , were computed by Equation (21) using the experimental data and plotted as a function of upstream Froude number in Figure 21. The data obtained from this study are compared with data measured by Ead and Rajaratnam [15], Izadjoo and Bejestan [14] and Samadi-Boroujeni et al. [38] to clarify the effect of the expansion ratio on the shear stress coefficient. The present data are compared with the results obtained from Equations (38) and (39). The following shear stress coefficient equations are also proposed by Izadjoo and Bejestan [14] and Samadi-Boroujeni et al. [38] on the rough bed, respectively.

$$\varepsilon = 0.058Fr_1^{3.035}, \quad R^2 = 0.9433 \quad (40)$$

$$\varepsilon = 0.428Fr_1^{2.256}, \quad R^2 = 0.93 \quad (41)$$

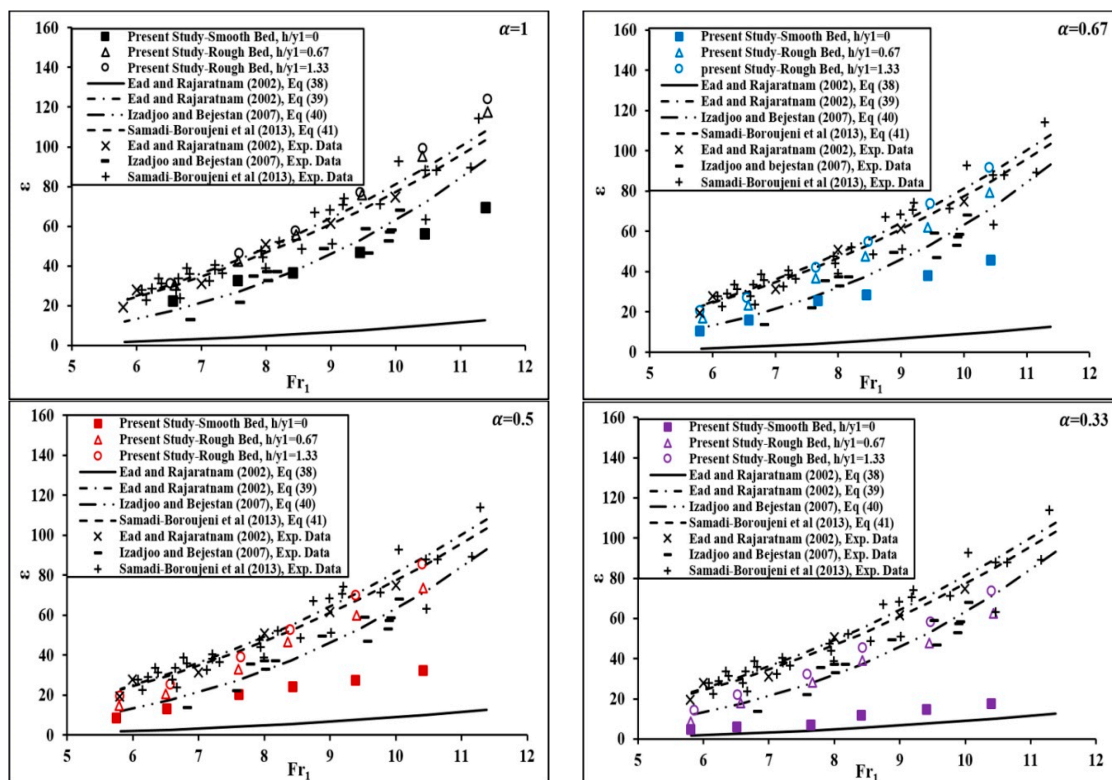


Figure 21. The bed shear stress coefficient as a function of upstream Froude number for two relative roughness heights ($h/y_1 = 0.67$ and 1.33) and different expansion ratios ($\alpha = 0.33, 0.5, 0.67, 1$) with asymmetry ratio of $\Delta = 0.16$.

As it can be seen from Figure 21, the results obtained from this study are in close agreement with the results determined by Ead and Rajaratnam [15], Izadjoo and Bejestan [14] and Samadi-Boroujeni et al. [38]. According to Figure 21, it is apparent that increase of the upstream Froude number causes the bed shear force index to increase nonlinearly due to the creation of large eddies within the jump for all the experiments. In addition, Figure 21 indicates that the value of ε in the hydraulic jump on rough beds is increased compared with the smooth bed in all expansion ratios. Furthermore, the roughness height of 2.8 cm is more effective in creating high turbulence, force and increasing the coefficient of bed shear force. The average values of the coefficient of the bed shear stress for different expansion ratios α (1, 0.67, 0.5 and 0.33) and the relative roughness height ($h/y_1 = 1.33$) were determined to be 10.49, 10.02, 9.46 and 7.78 respectively.

4. Conclusions

The stilling basin design and its dimensions are an important economic factor and using bed appurtenances and changing in cross sections and plan of basins can be beneficial to manage and reduce the construction cost. In this research, the effects of the expansion and the roughness height on the main properties of the jump were assessed through experimental investigation. The study revealed that the main parameters of the jump are a function of the upstream Froude number. It is noteworthy to mention, the bed roughness enhanced the energy dissipation by generation of large eddies and subsequently increased the bed shear stress and decreased the asymmetry and stabilized the hydraulic jump. Experimental observations showed that the spatial jump on an abrupt expanding basin is asymmetric and unstable, especially at high upstream Froude numbers, which brings about major difficulties in the hydraulic jump control.

In the present study, the proposed equations can be used for calculating the characteristics of hydraulic jump in the sudden asymmetric expanding stilling basin with roughened bed for a range of the upstream Froude numbers (Fr_1) from 5 to 11 and expansion ratios of $\alpha = 0.33, 0.5, 0.67$ and 1 with asymmetry ratio of $\Delta = 0.16$. The empirical equations were presented to show the effect of roughness and expansion ratios in different upstream Froude numbers on the jump characteristics and estimate the conjugate depth ratio (y_2/y_1), the relative length of the jump (L_j/y_1) and the relative roller length (L_r/y_1) and the relative energy loss (E_L/E_1). It was revealed from the experimental results that the required tailwater depth to form a jump is extremely reduced by asymmetry of the expanding channel and increase of the roughness elements ratio. Also, the conjugate depth ratio is enhanced with the increase of upstream Froude number and expansion ratio. The maximum decrement of conjugate depth is occurred in the expansion ratio of $\alpha = 0.33$ with the relative roughness height of $h/y_1 = 1.33$. The relative length and roller length ratio of the jump is increased as the channel width and upstream Froude number increased and is decreased as the relative roughness height increased. The results showed that the energy dissipation efficiency of the spatial jump in abruptly expanded stilling basin with roughened bed is greater than the classical jump. The asymmetry of the expanding channel also increased the relative energy loss due to creation of large eddies and presence of high turbulence along the basin. It is further concluded that the roughness height of 2.8 cm is more effective in increasing the coefficient of shear force in all expansion ratios.

As a resultant, the sudden asymmetric expanding basin with discrete roughness elements over the bed not only increased the efficiency in dissipating additional energy and reduced the sequent depth as well as the basin length, but also had significant influence on the formation of symmetric flows downstream of the basin.

Author Contributions: N.T., A.H.D. and F.S. designed and supervised the experiments. N.T. conducted the experimental measurements. N.T., A.H.D. and A.A. carried out the analysis and interpretation on the experimental data. N.T. wrote the paper. A.H.D. edited the manuscript. All authors read and confirmed the final manuscript.

Funding: This research received no external funding.

Acknowledgments: The authors would like to thank research vice-chancellor of University of Tabriz (IRAN) for financial support during the present research work. The writers are thankful to Adak Company for building the experimental arrangement.

Conflicts of Interest: The authors declare no conflict of interest.

Notations

The following symbols are used in this paper:

Fr_1	Upstream Froude number
Re_1	Upstream Reynolds number
α	Expansion ratio
b	Upstream channel width
B	Downstream channel width
Z	Distance between leftline of the main channel and the narrow section
Δ	Asymmetry ratio
y_1	Supercritical depth of the hydraulic jump
y_2	Sequent depth of the jump
y_2^*	Sequent depth of the classical jump
V_1	Mean velocity upstream of the jump
V_2	Mean velocity downstream of the jump
g	Gravitational acceleration
Y	Conjugate depth ratio of the hydraulic jump
Y^*	Conjugate depth ratio of the classical jump
D	Non-Dimensional depth deficit
E_1	Specific energy upstream of the jump
E_2	Specific energy downstream of the jump
E_L	Energy head loss of the hydraulic jump
E_L/E_1	Relative energy loss of the jump
η^*	Efficiency of the classical jump
η	Efficiency of the jump
L_j	Length of the jump
L_j^*	Length of the classical jump
L_r	Roller length of the jump
L_j/y_1	Relative length of the jump
L_r/y_1	Relative roller length of the jump
F_{P1}	Pressure force at the upstream of the jump
F_{P2}	Pressure force at the downstream of the jump
M_1	Momentum flux at the toe of the jump
M_2	Momentum flux at the end of the jump
F_e	Pressure force on the expanding basin
F_τ	Integrated bed shear stress of the jump
h	Height of the roughness element
h/y_1	Relative height of the roughness element
q	Discharge per unit width
ρ	Water density
ν	Kinematic viscosity of water
R^2	Coefficient of determination
ε	Shear stress coefficient

References

1. Hager, W.H. *Energy Dissipators and Hydraulic Jump*; Springer Science and Business Media: Dordrecht, Netherlands, 1992; Volume 8.
2. Chanson, H. *Energy Dissipation in Hydraulic Structures*; Taylor and Francis: London, UK, 2015.
3. Chanson, H. Development of the Bélanger equation and backwater equation by Jean-Baptiste Bélanger (1828). *J. Hydraul. Eng.* **2009**, *135*, 159–163. [[CrossRef](#)]
4. Hager, W.H. Classical hydraulic jump: Free surface profile. *Can. J. Civ. Eng.* **1993**, *20*, 536–539. [[CrossRef](#)]
5. Carollo, F.G.; Ferro, V.; Pampalone, V. New solution of classical hydraulic jump. *J. Hydraul. Eng.* **2009**, *135*, 527–531. [[CrossRef](#)]
6. Gill, M. Effect of boundary roughness on hydraulic jump. *Water Power Dam Constr.* **1980**, *32*, 22–24.
7. Peterka, A.J. *Hydraulic Design of Stilling Basins and Energy Dissipators*; United States Department of the Interior, Bureau of Reclamation: Denver, CO, USA, 1958.

8. Rajaratnam, N. The Hydraulic Jump as a Well Jet. *J. Hydraul. Division* **1965**, *91*, 107–132.
9. Hager, W.H.; Bremen, R. Classical hydraulic jump: Sequent depths. *J. Hydraul. Res.* **1989**, *27*, 565–585. [[CrossRef](#)]
10. Hager, W.H.; Bremen, R.; Kawagoshi, N. Classical hydraulic jump: Length of roller. *J. Hydraul. Res.* **1990**, *28*, 591–608. [[CrossRef](#)]
11. Wu, S.; Rajaratnam, N. Free jumps, submerged jumps and wall jets. *J. Hydraul. Res.* **1995**, *33*, 197–212. [[CrossRef](#)]
12. Chanson, H. Hydraulic jumps: turbulence and air bubble entrainment. *J. Houille Blanche* **2011**, *3*, 5–16. [[CrossRef](#)]
13. Rajaratnam, N. Hydraulic jumps on rough beds. *Trans. Eng. Inst. Can.* **1968**, *11*, 1–8.
14. Izadjoo, F.; Shafai Bejestan, M. Corrugated bed hydraulic jump stilling basin. *J. App. Sci.* **2007**, *7*, 1164–1169.
15. Ead, S.; Rajaratnam, N. Hydraulic jumps on corrugated beds. *J. Hydraul. Eng.* **2002**, *128*, 656–663. [[CrossRef](#)]
16. Hughes, W.C.; Flack, J.E. Hydraulic jump properties over a rough bed. *J. Hydraul. Eng.* **1984**, *110*, 1755–1771. [[CrossRef](#)]
17. Carollo, F.G.; Ferro, V.; Pampalone, V. Hydraulic jumps on rough beds. *J. Hydraul. Eng.* **2007**, *133*, 989–999. [[CrossRef](#)]
18. Pagliara, S.; Lotti, I.; Palermo, M. Hydraulic jump on rough bed of stream rehabilitation structures. *J. Hydro-Environ. Res.* **2008**, *2*, 29–38. [[CrossRef](#)]
19. Abbaspour, A.; Hosseinzadeh Dalir, A.; Farsadizadeh, D.; Sadraddini, A.A. Effect of sinusoidal corrugated bed on hydraulic jump characteristics. *J. Hydro-Environ. Res.* **2009**, *3*, 109–117. [[CrossRef](#)]
20. Afzal, N.; Seena, A.; Bushra, A. Analysis of turbulent hydraulic jump over a transitional rough bed of a rectangular channel: universal relations. *J. Eng. Mech.* **2011**, *137*, 835–845. [[CrossRef](#)]
21. Mossa, M. On the oscillating characteristics of hydraulic jumps. *J. Hydraul. Res.* **1999**, *37*, 541–558. [[CrossRef](#)]
22. Ben Meftah, M.; Mossa, M.; Pollio, A. Considerations on shock wave/boundary layer interaction in undular hydraulic jumps in horizontal channels with a very high aspect ratio. *Eur. J. Mech. B Fluids* **2010**, *29*, 415–429. [[CrossRef](#)]
23. De Padova, D.; Mossa, M.; Sibilla, S. 3D SPH modeling of hydraulic jump in a very large channel. *J. Hydraul. Res.* **2013**, *51*, 158–173. [[CrossRef](#)]
24. De Padova, D.; Mossa, M.; Sibilla, S. SPH modeling of hydraulic jump oscillations at an abrupt drop. *Water* **2017**, *9*, 790. [[CrossRef](#)]
25. De Padova, D.; Mossa, M.; Sibilla, S. SPH numerical investigation of characteristics of hydraulic jumps. *Environ. Fluid Mech.* **2018**, *18*, 849–870. [[CrossRef](#)]
26. Hager, W.H. Hydraulic jump in non-prismatic rectangular channels. *J. Hydraul. Res.* **1985**, *23*, 21–35. [[CrossRef](#)]
27. Bremen, R. Expanding stilling basin. Ph.D Thesis, Ecole Polytechnique Federale de Lausanne (EPFL), Lausanne, Switzerland, 1990.
28. Herbrand, K. The Spatial hydraulic jump. *J. Hydraul. Res.* **1973**, *11*, 205–218. [[CrossRef](#)]
29. Bremen, R.; Hager, W.H. T-jump in abruptly expanding channel. *J. Hydraul. Res.* **1993**, *31*, 61–78. [[CrossRef](#)]
30. Alhamid, A.A. S-jump characteristics on sloping basins. *J. Hydraul. Res.* **2004**, *42*, 657–662. [[CrossRef](#)]
31. Zare, H.K.; Doering, J.C. Forced Hydraulic Jumps below Abrupt Expansions. *J. Hydraul. Eng.* **2011**, *137*, 825–835. [[CrossRef](#)]
32. Hassanpour, N.; Hosseinzadeh Dalir, A.; Farsadizadeh, D.; Gualtieri, C. An experimental study of hydraulic jump in a gradually expanding rectangular stilling basin with roughened bed. *Water* **2017**, *9*, 945. [[CrossRef](#)]
33. Agarwal, V. Graphical solution to the problem of sequent depth and energy loss in spatial hydraulic jump. In *Proceedings of the Institution of Civil Engineers-Water and Maritime Engineering*; Thomas Telford Ltd.: London, UK, 2001.
34. Bejestan, M.S.; Neisi, K. A new roughened bed hydraulic jump stilling basin. *Asian J. App. Sci.* **2009**, *2*, 436–445. [[CrossRef](#)]
35. Mohamed Ali, H.S. Effect of roughened bed stilling basin on length of rectangular hydraulic jump. *J. Hydraul. Eng.* **1991**, *117*, 83–93. [[CrossRef](#)]
36. USBR. *Research Studies on Stilling Basins, Energy Dissipators and Associated Appurtenances*; United States Department of the Interior, Bureau of Reclamation: Denver, CO, USA, 1955; Volume 399.

37. Carollo, F.G.; Ferro, V.; Pampalone, V. New Expression of the Hydraulic Jump Roller Length. *J. Hydraul. Eng.* **2012**, *138*, 995–999. [[CrossRef](#)]
38. Samadi-Boroujeni, H.; Ghazali, M.; Gorbani, B.; Fattahi Nafchi, R. Effect of triangular corrugated beds on the hydraulic jump characteristics. *Can. J. Civ. Eng.* **2013**, *40*, 841–847. [[CrossRef](#)]



© 2019 by the authors. Licensee MDPI, Basel, Switzerland. This article is an open access article distributed under the terms and conditions of the Creative Commons Attribution (CC BY) license (<http://creativecommons.org/licenses/by/4.0/>).